Algerian Democratic Republic and Populaire

Ministry of Higher Education

and scientific research

Echahid Hamma Lakhder University of El-Oued

Faculty of Technology

Thesis presented for obtaining the

ACADEMIC MASTERS

Domain: Science and Technology

Sector: Mechanical Engineering

Specialty: Mechanical Renewable Energy

Theme:

Design and Simulation of Wind Turbine Spiral Blade Liam F1

Before the jury composed of:

Gherbi med taher	Président
Mencer nour eddinne	Examiner
Dr : DEGHOUM Khalil	Farmer

Presented by:

- Bouhania Faycal
- BenFerdjallah Tahar
- Benchabana Med Larbi

AnnéeAcadémique2023-2024

Dedication

We dedicate this work:

To all families

Acknowledgement

We thank Almighty God for giving me the courage, will and patience to complete this dissertation.

We warmly thank Professor **Dr. DEGHOUM Khalil**, Lecturer at the University of El Oued, for the honor he did me by accepting to supervise my dissertation.

Thank you to everyone who helps us in this work a little or a lot

All my thanks and appreciation to all the teachers of the mechanical engineering department.

Abstract

The ultimate objective of this work concerns to deepen knowledge about the world of wind turbines, specifically Archimedes Spiral-type wind turbines. The first step is to give general information about wind turbines. Subsequently, Archimedes Spiral wind turbines are referred to as dynamic and static notions. After that, we use a computer-aided design of a model that is proposed for it to be manufactured and tested in future works. Finally, we finish with a static and dynamic simulation on SolidWorks to prevent performances to be confirmed theoretically in future projects.

Résumé

L'objectif ultime de ce travail concerne l'approfondissement des connaissances surlemondedes éoliennes, notamment les éoliennes de type Archimède Spirale. La première étapeconsiste à donner des informations générales sur les éoliennes. Par la suite, les éoliennes Archimède Spiral sont décrites comme des notions dynamiques et statiques. Après cela, nous utilisons une conception assistée par ordinateur d'un modèle qu'il est proposé de fabriquer et de tester dans des travaux futurs. Enfin, nous terminons par une simulation statique et dynamique sur SolidWorks pour éviter que les performances ne soient confirmées théoriquement dans les projets futurs.

خلاصة

الهدف النهائي لهذا العمل يتعلق بتعميق المعرفة حول عالم توربينات الرياح، ولا سيما توربينات الرياح من النوع الحلزوني لأرخميدس. الخطوة الأولى هي إعطاء معلومات عامة عن توربينات الرياح. وفي وقت لاحق، تم وصف توربينات الرياح الحلزونية لأرشيميد بأنها مفاهيم ديناميكية وثابتة. بعد ذلك، نستخدم تصميمًا بمساعدة الكمبيوتر للنموذج المقترح تصنيعه واختباره في العمل المستقبلي. أخيرًا، ننتهي بمحاكاة ثابتة وديناميكية على برنامج SolidWorks لتجنب تأكيد الأداء نظريًا في المشاريع المستقبلية.

LIST OF Nomenclature

U∞	free stream velocity [m/s]
A	Swept area[m ^{2}]
Cp	Power coefficient [-]
Cd	Drag Coefficient P Power [-]
d	Shaft diameter [W]
D	Rotor diameter [m]
R	Rotor radius Re Reynolds number [m]
λ	Tip speed ratio [m]
L	Blade length [-]
T	Torque [N-m]
ω	Angular velocity [rad/s]
n	Factor of Safety [-]
Sut	Ultimate tensile stress [MPa]
Sy	Yield stress [MPa]
C10	Dynamic load rating [-]
C0	Static load rating [-]
ρ	Density of air [kg/m ^{3}]
C	f Skin friction coefficient [-]
τ	Shear Stress [Pa]
Ufric	Frictional velocity [m/s]
Δs	First cell height [m]
Y+	Non-dimensional wall distance [-]
t	Blade thickness [m]
θ	Opening angle [degrees (°) or radians (rad)]
u	Velocity in X-direction [m/s]
v	Velocity in Y-direction [m/s]
w	Velocity in Z-direction [m/s]
p	Pressure [Pa]
m/s	Meter per second [m/s]
N-m	Newton meter [N-m]
Pa	Pascal [Pa]
MPa	Mega Pascal [MPa]
kN	Kilo Newton [kN]
rad/s	Radian per second [rad/s]
W	Watt [W]
kW	Kilo watt [KW]
MW	Megawatt [MW]
TWh	Tera watt hour [TWh]
Rpm	Revolutions per minute [Rpm]

List of Figures:

List of table

Summary

General Introduction

General Introduction

Renewable energies like solar, wind, and hydropower offer inexhaustible, clean energy that can be self-managed. They stand as the ultimate solution to combat the use of fossil fuels, which contribute to global warming and pollution. Consequently, substantial advancements in renewable energy development are necessary to replace fossil fuels. Presently, the wind energy sector is witnessing a surge in advanced research aimed at enhancing its efficiency. Integrating renewable energies into energy policies has become essential for sustainable development and addressing the challenges posed by the current global energy landscape. It is in response to this imperative that we undertook the present work.

Wind energy, as a renewable source, fosters diversification and energy independence. It is environmentally friendly, emitting no greenhouse gases, and its machinery has a favorable life cycle impact on the environment. Additionally, wind energy is decentralized, bringing power generation closer to consumers. These qualities have made it a recommended choice by public authorities and a pivotal component of future energy strategies as an alternative to fossil fuels.

A wind turbine, which converts wind's kinetic energy into electrical energy, plays a central role in harnessing wind power. By 2020, wind farms worldwide were generating over 650 gigawatts of power, with an annual addition of 60 gigawatts. Wind turbines have emerged as a crucial source of intermittent renewable energy, helping to reduce energy costs and diminish reliance on fossil fuels in many countries. Studies indicate that wind energy boasts the lowest relative greenhouse gas emissions, minimal water consumption demands, and the most favorable social impacts compared to other energy sources like photovoltaic, hydro, geothermal, coal, and gas.

Wind turbines come in various sizes and configurations, primarily horizontal or vertical axes, with horizontal being the predominant type. They serve a spectrum of purposes, from charging batteries to powering remote devices like traffic warning signs. Moreover, larger turbines can contribute to domestic power supplies while enabling the sale of excess power back to utility suppliers through the electrical grid.

This memorandum outlines the preliminary design of an Archimedean spiral-type wind turbine, a promising variant of horizontal axis wind turbines (HAWT). The design is based on calculations and observations of various geometric parameters, aided by computational fluid dynamics (CFD) analysis, followed by fabrication and testing.

The first chapter addresses the origin of use of wind energy, we then move on to the definition and classification of wind turbines then the mode of operation of wind turbines, to end with the global and national situation of wind energy.

Then we discuss the study of turbines Archimedean spiral-type wind turbine, one of the emerging HAWT, with the aid of calculations and the observations of various geometric parameters by CFD analysis along with its fabrication and testing.

The second chapter outlines the methods used in a Computational Fluid Dynamics (CFD) study of a mobile Archimedes wind turbine with Ansys. It begins with analyzing various turbine designs in simulation software, followed by assessing their aerodynamic properties under uniform wind speeds to find the optimal model

The third chapter process of simulation entails replicating complex real-world physical phenomena using computers or networks. Scientific numerical simulations utilize theoretical models to analyze the behavior and attributes of simulated systems, enabling the prediction of their evolution. This involves numerical calculations, with graphical interfaces enabling the visualization of results through synthetic images. The term "digital" denotes the execution of computer programs.

Chapter I

Generalities about wind energy

Introduction

The aim of this chapter is to enhance our fundamental understanding of wind turbines. We'll start with a concise overview of the historical utilization of wind as an energy source. Next, we'll delve into defining and categorizing wind turbines based on their configurations, particularly focusing on rotor position. We'll then explore the operational principles of vertical axis wind turbines, with a spotlight on the Savonius type. Finally, we'll assess the worldwide and national contexts of wind turbines and examine their environmental impacts.

I.1 Origins of wind turbines

The historical origins of wind turbines are subject to conflicting interpretations. Some scholars suggest that the use of wind energy traces back to approximately 5000 years BCE, coinciding with the advent of sailing. They attribute the earliest form of wind turbines to the windmills crafted from stone by the ancient Egyptians near Alexandria, around 3000 years ago [1].

The earliest reliable historical documentation regarding wind turbines dates back to around 664 BCE [2], originating in the Persian region of "SEISTAN" (currently bordering Afghanistan). These early windmills were constructed from wood and fabric and served the purposes of grain milling and water pumping. Figure 1.1 depicts a wind turbine operating on this principle, showcasing a vertical axis design driven by the wind's thrust force.

Figure I-1: Vertical-axis windmill for grain milling, Afghanistan [3]

The adoption of windmills spread extensively across the Middle East and Central Asia, later reaching China and India [3]. In Europe, windmills made their debut during the early Middle Ages. Initially employed for grain milling and water pumping, hence earning the moniker "mills," these windmills featured four blades rotating around a horizontal axis.

In 1887, American scientist Charles F. Brush, hailing from Cleveland, Ohio, erected the inaugural wind turbine. Standing at a height of 17 meters, it boasted 144 cedar blades and delivered a power output of 12 kW. Another account credits Professor James Blyth of Anderson

College in Glasgow, Scotland, with constructing the first windmill for electricity generation in the same year [4]. In 1890, Danish innovator Poul La Cour introduced the inaugural "industrial" wind turbine designed for electricity generation. Subsequently, in 1920, French engineer Georges JM Darrieus introduced the concept of the Darrieus wind turbine, characterized by its vertical axis rotor. As the demand for energy escalated and technological advancements in large wind turbines progressed, Denmark marked a significant milestone in 1971 with the establishment of its first offshore wind farm boasting a total capacity of 5 MW.

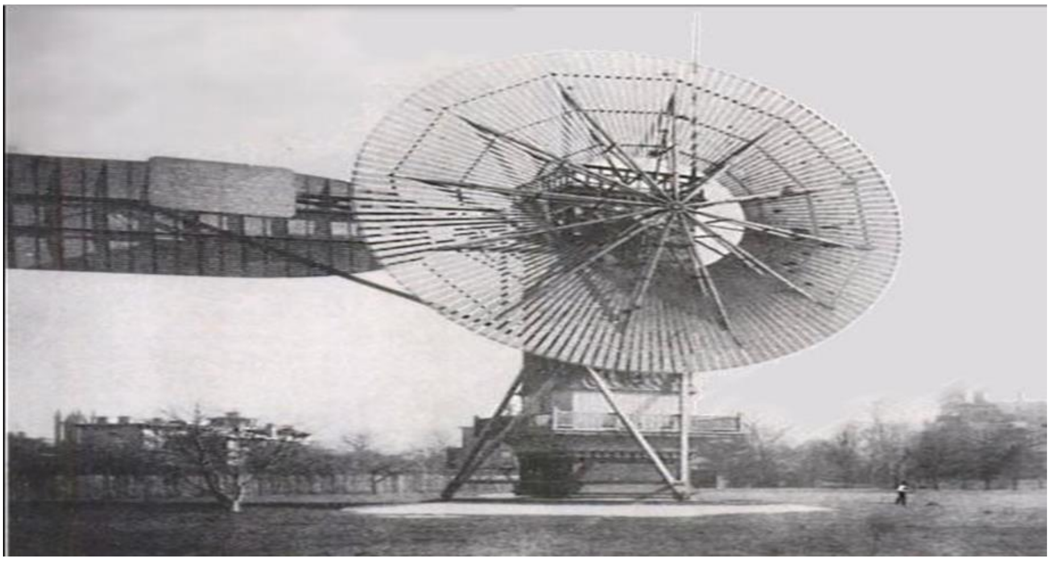

Figure I-2: first wind turbine designed by chale.F.Brush [4].

I.2 Wind energy

A wind turbine, often referred to as a wind generator, is a mechanism that converts a portion of the kinetic energy from the wind, which is a moving fluid, into mechanical energy accessible through a transmission shaft. This mechanical energy is then further transformed into electrical energy through the operation of a generator.

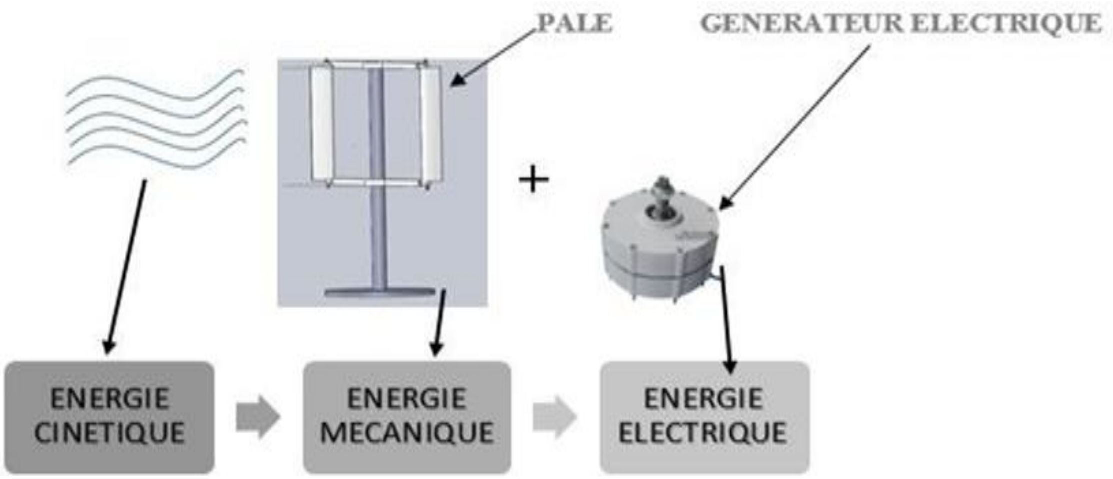

Figure I-3 Wind kinetic energy conversion [5]

Wind power is an energy resource reliant on the movement of the wind. It derives indirectly from the sun, as wind is generated by variations in pressure and temperature within the atmosphere due to solar radiation. Consequently, air masses set into motion as a result. The movement of air masses results in the accumulation of kinetic energy [5], which can be harnessed and utilized for various purposes:

- Conversion into mechanical energy
- Conversion into electrical energy

This energy source presents two significant advantages: it is entirely clean and renewable. During its utilization, it generates no emissions, radiation, or toxic byproducts (thus, no greenhouse effect) and produces no waste. However, its primary drawback lies in its lack of flexibility and its variability, particularly its reduced performance during turbulent wind conditions [5].

I.3 The different types of wind turbines

Wind turbines are broadly categorized into two main types based on the orientation of the shaft supporting the blades: Horizontal Axis Wind Turbines (HAWTs) and Vertical Axis Wind Turbines (VAWTs). HAWTs, which feature blades rotating around a horizontal axis, are the predominant choice for large-scale wind power generation. Meanwhile, VAWTs, with blades spinning around a vertical axis, have gained traction more recently, particularly for smaller-scale applications in urban or residential settings. Although VAWT technology is relatively newer, it is undergoing rapid development, with a growing number of projects catering to both small and medium power needs, including initiatives for larger VAWTs as well.

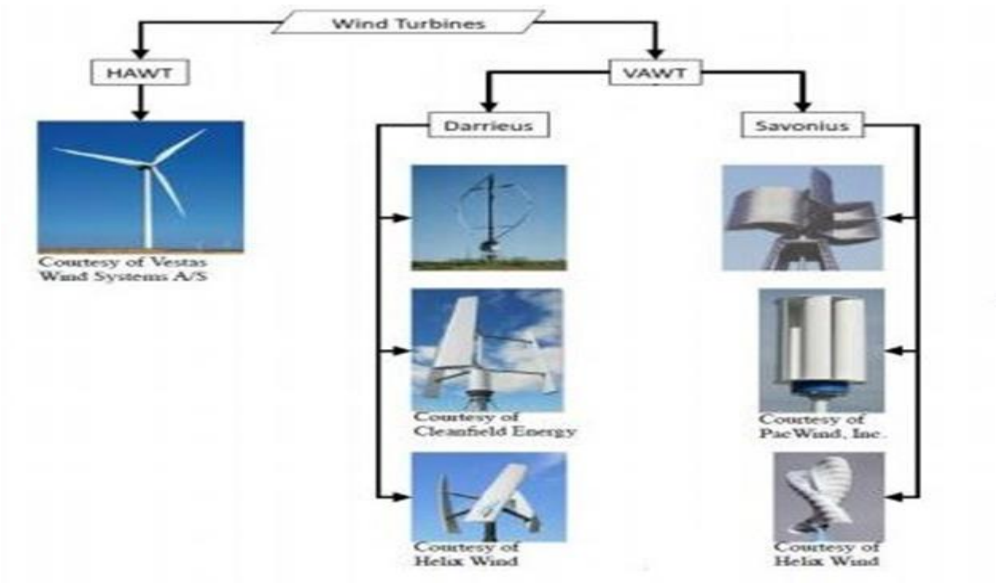

Figure 1-4: The different types of wind turbines [6]

I.3.1 Horizontal axis wind turbines

Horizontal axis wind turbines (HAWTs) draw on the technology of traditional windmills. They have demonstrated efficiency and are generally more effective than vertical axis wind turbines, although their efficiency decreases in high-speed laminar winds. However, they exhibit poor performance in unstable wind conditions or when wind direction is uncertain. HAWTs utilize airfoils and operate based on lift force. The number of blades employed for electricity generation typically ranges from 1 to 3, with the three-blade configuration being the most prevalent. This choice represents a balance between factors such as the power coefficient (which is approximately 5% lower with a three-blade compared to a two-blade configuration), cost considerations, and wind rotation speed. Wind turbines of this type are characterized by their ability to harness the full power spectrum of the wind [6]. Key features include:

- Maximum power coefficient: Approximately 45-50%.
- Optimal specific speed: Typically ranging from 5 to 6.
- Starting speed: Initiation occurs at speeds of 4-5m/s.

Figure I-5: Horizontal axis wind turbine [7]

Two types of configurations are commonly encountered in wind turbines: "upstream" and "downstream". In "upstream" wind turbines, the blades are positioned on the side of the tower that faces the wind, whereas in "downstream" wind turbines, the blades are situated on the opposite side.

Each configuration presents its own set of advantages and disadvantages. The "upstream" setup necessitates rigid blades to prevent any risk of collision with the tower, whereas the "downstream" configuration allows for the use of more flexible rotors. Additionally, in an "upstream" machine, the airflow over the blades experiences minimal disruption from the presence of the tower. On the other hand, a downstream machine is theoretically self-orienting in accordance with the wind direction, while an "upstream" wind turbine typically requires specific orientation mechanisms.

It is worth noting that the majority of large-scale wind turbines for power generation adopt the "upstream" configuration [8].

Figure I-6: Type of sail mounting [8]

Currently, horizontal axis wind turbines dominate the commercial market. The largest of these turbines boast heights reaching up to 180 meters at the tip of the blade, supported by a 120-meter hub, and are capable of generating 6 megawatts of power.

I.3.2 Vertical axis wind turbines Vertical axis wind turbines

Vertical axis wind turbines (VAWTs) are better suited for urban environments due to their ability to operate independently of wind direction, which is often unpredictable in such settings. Additionally, VAWTs tend to be more robust and less noisy compared to horizontal axis wind turbines (HAWTs). However, the optimal design for VAWTs, especially in urban contexts, has not been definitively established as no single model has emerged as the most efficient. Numerous technological variations have been explored, but only two structures, the Darrieus rotor and the Savonius rotor, have progressed to the industrialization stage.

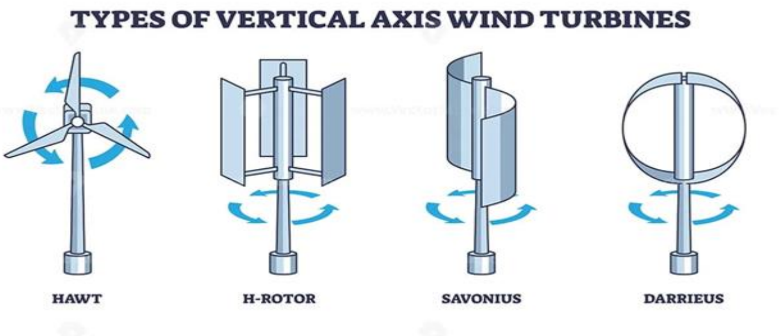

Figure I-7: vertical axis wind turbine[6]

I.4 Global wind energy production

The World Wind Energy Association (WWEA) has compiled data on new wind power installations during the initial six months of 2022. Through a survey conducted among WWEA's member associations worldwide, estimates of global installations as of the present and projections for the conclusion of 2022 have been made available Comparing the figures, it is noted that while 27.6 Gigawatts were added in the first half of 2021, the world saw an increase to 28.9 Gigawatts during the corresponding period in 2022. This translates to an annual growth rate of 13% when comparing the total installed capacity at the end of June 2022 with that of June 2021. Consequently, the global installed capacity reached 874 Gigawatts by June 2022 [9].

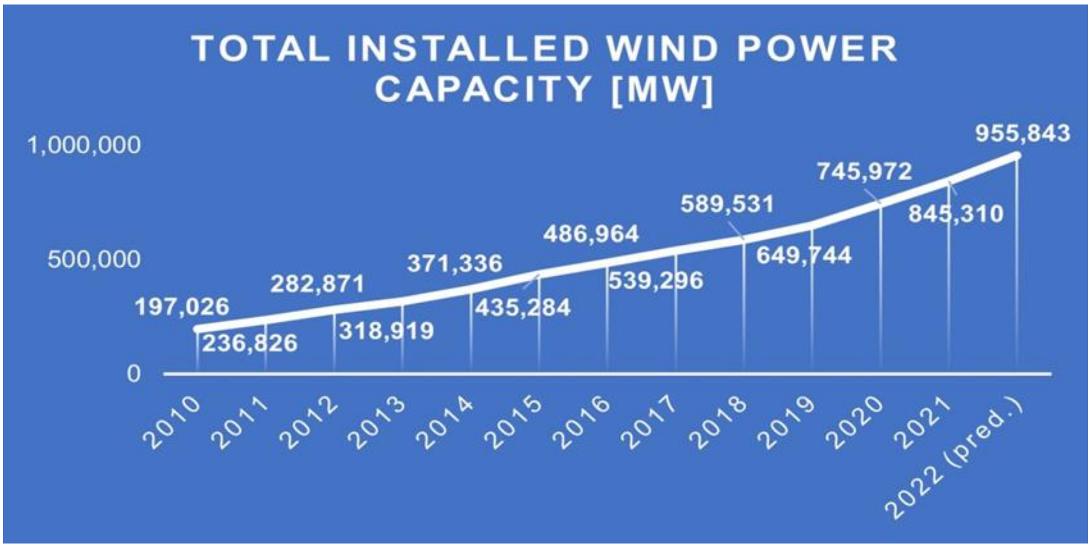

Figure I-8: total installed wind power capacity (MW) [9].

Anticipated momentum is foreseen for the latter half of 2022. As per the estimations provided by our members, the World Wind Energy Association (WWEA) anticipates a total addition of new capacity reaching at least 110 Gigawatts for the entirety of 2022. This projection signifies a new all-time high, surpassing the previous year's figure of 100 Gigawatts in 2021.

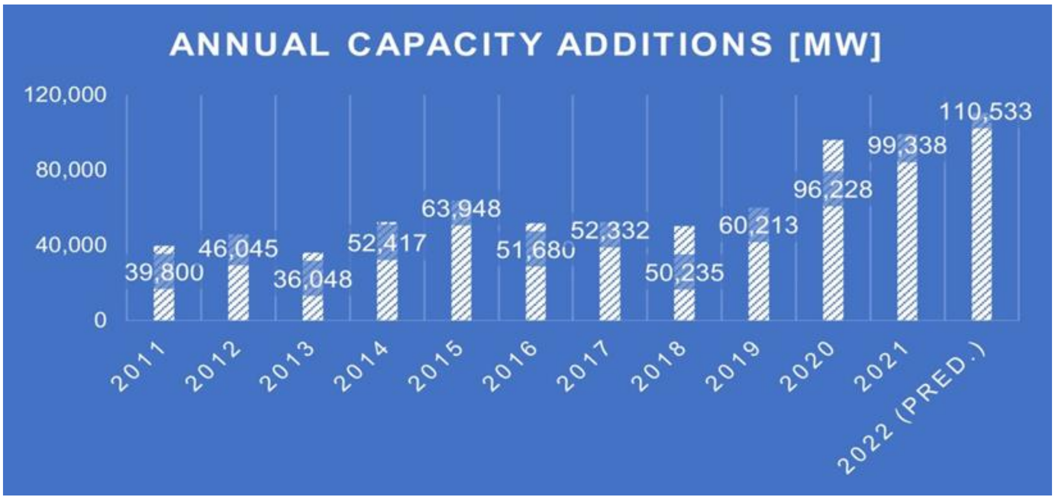

Figure I-9: annual capacity additions (MW) [9].

As a result, the global installed wind capacity is projected to exceed 955 Gigawatts by the conclusion of 2022, and is forecasted to surpass the milestone of 1 million Megawatts by mid-2023.

China is expected to once again dominate the market, with an anticipated installed capacity of 60 Gigawatts. Furthermore, robust growth is anticipated in other key markets, such as the United States, although it may not reach the levels seen in 2021. Spain is poised to emerge as the largest European market in 2022, while Brazil is expected to maintain its position as the leader in South American wind power.

Table I.1WWEA Annual Report 2022

Rank	Country/ Region	Dec2022 (predicted)	juin-22	New capacity 1-6-2022	dec21	juin-21	dec20
1	China	406.670	359.770	13.100	346.670	301.750	290.750
2	United States	145.945	139.145	3.798	135.347	129.283	122.328
3	Germany	66.966	64.642	718	63.924	63.542	62.708
3	India	41.600	40.900	1.100	39.800	39.600	38.625
4	Spain	33.073	29.512	982	28.530	27.977	27.446
5	United	NA	27.700	1.952	25.748	24.876	24.458
6	brazil	26.466		197		19.100	
7	France	NA	20.036	952	19.084	18.310	17.949
8	Canada	16.000	15.152	848	14.304	NA	13.627
9	Sweden	14.511	13.252	1.155	12.097	NA	9.922
10	Italy	11.600	11.400	100	11.300	11.000	10.850
	Rest of the World (estimated 2022)	193.012	130.639	3.970	126.669	138.093	109.300
	Total	955.843	874.182	28.872	845.310	773.531	745.972

WWEA President Hon. Peter Rae AO from Australia remarks, "While world leaders convene at the COP in Egypt to explore more effective strategies for combatting climate change through international agreements, the global wind energy sector continues to offer tangible solutions. Moreover, if governments continue to enhance the legal frameworks governing wind power deployment and operation, the growth of wind power can be further accelerated."

WWEA Secretary General Stefan Gsänger adds, "It is important to underscore that the promising increase in growth rates witnessed in mid-2022 is not solely attributable to the response to the Russian war against Ukraine and the resulting challenges in fossil energy supply and pricing. With many governments now implementing new policies to expedite the deployment of wind power, we anticipate additional momentum in the coming years."

I.5 Wind Energy Perspective:

In November 2016, the Paris Agreement was officially ratified by 55 countries, collectively responsible for at least 55% of global greenhouse gas emissions, thereby bringing it into effect. This signifies a global commitment to limiting global warming to below 2°C, ideally below 1.5°C, over the next century. Wind energy is poised to play a crucial role in achieving this objective.The Global Wind Energy Council (GWEC) anticipates robust and sustained growth in wind capacity until 2020, averaging at 13% per year. This growth trajectory is expected to result in a total of 792.1 gigawatts (GW) of newly installed capacity, representing an 80% increase compared to 2015 figures. The main driver of this expansion is projected to be Asia, where wind capacity is forecasted to double, reaching 353 GW.This optimistic scenario, as envisioned by GWEC, is contingent upon significant reductions in the installation and production costs of wind energy. A key factor in this equation is the anticipated decline in turbine prices, which have already decreased by a third since 2009.

Additionally, the International Renewable Energy Agency (IRENA) estimates that onshore wind power could further reduce its costs by 26% by 2025 [10].

I.6 Wind energy in Algeria:

In Algeria, the initial endeavor to integrate wind turbines into the electrical energy distribution network traces back to 1957. This initiative involved the installation of a 100 kW wind generator at the Grands Vents site in Algiers. Designed by French engineer ANDREAU, this prototype was originally situated in St-Alban, England. Standing at a height of 30 meters with a diameter of 25 meters, it featured a two-blade variable pitch pneumatic design. Subsequently, Electricity et Gaz d'Algérie procured this turbine, dismantled it, and reassembled it in Algeria [11].

Figure I-10: 100 kW wind turbine from Grand Vent [11]

Presently, the total installed wind power capacity in Algeria remains relatively insignificant. However, the country has taken strides in this area, with the establishment of its first wind farm boasting a capacity of 10 megawatts (MW) in Adrar. Additionally, the Ministry of Energy and Mines has outlined plans, as part of its Renewable Energy development program, to construct seven additional wind farms with a combined capacity of 260 MW in the medium term, with a target of reaching 1700 MW by 2030.

Furthermore, this program includes initiatives to initiate the industrialization of specific components of wind turbines, such as blades. It's worth noting that one of the earliest applications of wind energy in Algeria was for water pumping purposes. In 1953, the colonization and hydraulic services installed the largest pumping wind turbine in Adrar. This machine, mounted on a 25-meter-high mast and equipped with three 15-meter-diameter blades, operated for nearly a decade. More recently, the High Commission for the Development of the Steppe installed 77 water pumping wind turbines in the Highlands [11].

I.7 What are the impacts of wind turbines on the environment?

The impacts of wind turbines on the environment prompt multifaceted discussions. Let's delve into the positive aspects first: electricity production through wind turbines is environmentally friendly as it does not emit CO_2 or other harmful particles. However, the manufacturing process of wind turbines requires energy and can result in emissions, similar to the production of solar panels or nuclear power plants.

Furthermore, wind energy harnesses the inexhaustible force of the wind, unlike fossil resources such as gas or uranium for nuclear power, which adds another environmental advantage to wind power.

On the flip side, there are negative aspects often discussed. One Common concern is the impact on landscapes, as multiple turbines are required to generate sufficient electricity, occupying space and altering visual aesthetics. Additionally, noise pollution near wind turbines can be a source of disturbance.

Wind turbines also affect local flora and fauna, particularly birds and bats, which may collide with the moving blades due to their altitude. However, radar devices are now available to deter them from approaching the turbines. The biodiversity around wind turbines may also be affected, leading to specific areas being designated for turbine installation to mitigate these impacts.

Considering the lifespan and recycling of materials is also crucial, as with any energy production system. Wind turbines typically have a lifespan of around 20 years, after which parts or the entire turbine must be replaced. Recent models feature fewer mechanical parts, reducing friction and wear, which is a positive development for longevity.

Background on securing energy supply issues and addressing climate change:

To address energy supply concerns, combat climate change, reduce greenhouse gas emissions, protect biodiversity, and promote renewable technologies, energy conservation and efficiency enhancements have become increasingly imperative. Among renewable resources, wind energy stands as a well-established technology with significant potential for commercialization and large-scale production. The primary application of wind power is electricity generation through large grid-connected wind farms. However, as the power grid expands and electricity scarcity diminishes, small-scale wind turbines are now being utilized in various countries and sectors, including city road lighting, mobile communication base stations, offshore aquaculture, and seawater desalination.

In the context of Nepal, small-scale wind turbines have not received adequate attention despite their considerable potential and the country's growing energy challenges. Despite their size, these turbines could offer valuable assistance to Nepalese households.

I.8 Archimedes Spiral type Wind Turbine

The Archimedean Spiral-Type Wind Turbine (ASWT) is a small-scale horizontal axis wind turbine that follows the principles of the Archimedean spiral. It captures wind energy by redirecting its flow 90 degrees from its original direction. Unlike conventional horizontal axis wind turbines (HAWTs), which rely solely on lift force, the ASWT utilizes both lift and drag forces to harness wind power. This enables it to tap into the kinetic energy present in wind currents. Notably, the ASWT offers the advantage of operating efficiently even at low wind speeds.

I.9 Objective

I.9.1 General Objective

To design, conduct CFD analysis and develop a model of Archimedes spiral-type wind turbine.

I.9.2 Specific Objectives

1. Determine the optimal Archimedes wind turbine model through CFD analysis.
2. Construct a model suitable for the available wind tunnel.
3. Conduct wind tunnel testing on the fabricated model.
4. Compare the results obtained from wind tunnel testing with those obtained numerically.

I.10 Methodology

The methodology adopted during the project is described below:

I.11 Problem Statement

1. Existing small-scale wind turbines exhibit low efficiency, typically below 20 kW.
2. Horizontal axis wind turbines produce excessive noise levels, rendering them unsuitable for installation in residential areas.
3. Achieving maximum power coefficient necessitates a high tip speed ratio.

The fundamental challenge addressed by this project is to develop a cost-effective small-scale wind turbine tailored for regions experiencing wind velocities ranging between 3 m/s and 12 m/s. Such a turbine could effectively meet energy needs in areas lacking access to the national grid, as well as mitigate energy deficits resulting from load shedding in regions connected to the grid.

I.11.1 Literature Review

The literature review was conducted continuously throughout the project timeline until its conclusion. It encompassed web-based research, consultations with experts, and manual study. Specifically, literature pertaining to simulation and optimization was extensively examined online. Additionally, in-depth research was conducted to identify and analyze design parameter selection for the turbine. Previous studies and installations of turbines were also scrutinized to establish a foundation for the turbine utilized in the project.

I.11.2 Design

The process of selecting the most efficient design within the given constraints proceeded according to the following steps:

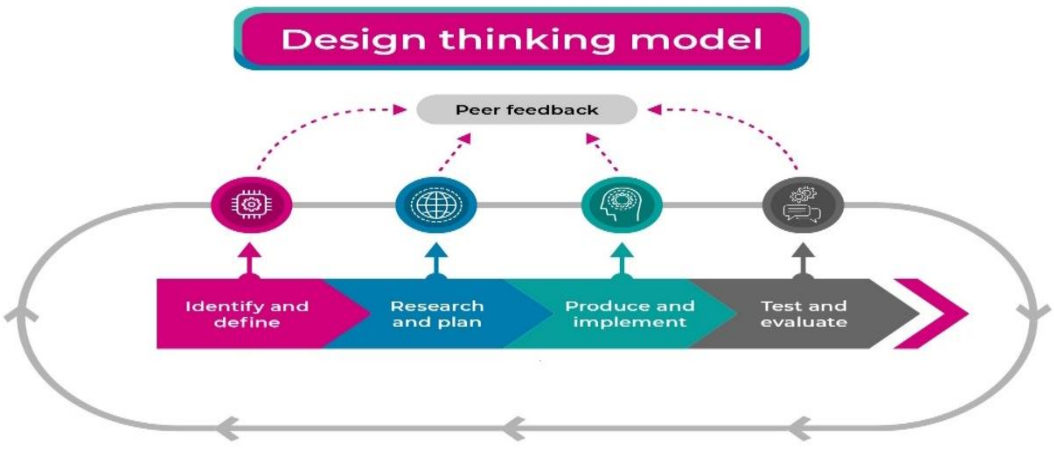

Figure I.11 Phases of design thinking [19]

I.11.3 Fabrication

The fabrication process involved utilizing a 3D printer to construct the turbine blade, while the shaft was manufactured separately. Subsequently, the frame was attached using suitable materials and integrated with the other components through appropriate processes, resources, and tools.

1.12 Scope of Work

The Archimedes wind turbine is designed to cater to households situated in areas with favorable wind speeds, allowing for the harnessing of available wind energy. Its compact size enables easy installation on rooftops, akin to solar panels, making it adaptable to various locations to meet daily energy requirements. Additionally, the turbine can serve multiple applications, including street lighting, functioning as a hybrid energy source in conjunction with solar panels to ensure consistent output, and serving as a backup source for various purposes.

I.13 Historical Background

Wind energy has been utilized for millennia, serving purposes such as grain milling and water pumping. Its historical roots can be traced back to the tenth century in Persia, marking the earliest recognized use of windmills [12]. Presently, there are hundreds of thousands of windmills in operation worldwide. Modern iterations are often referred to as wind turbines, a term reflecting their functional resemblance to steam and gas turbines and distinguishing them from traditional predecessors [13].

During the 1990s, wind energy experienced unprecedented growth, emerging as the fastest-growing energy technology in terms of installed capacity percentage annually [14]. However, this growth is not uniform across regions, with Europe leading in global wind energy capacity, followed by North America and Asia-Pacific [14].

Wind energy is poised to assume a progressively significant role in national energy landscapes [15, 16]. Wind turbines function by converting the kinetic energy of the wind into electrical energy through blade rotation. Greenpeace forecasts that wind could supply approximately 10% of electricity by 2020 [17].

In terms of costs, the manufacturing expenses for wind turbines in the 1990s declined by approximately 20% each time the number of turbines doubled. Presently, the production of large-scale, grid-connected wind turbines is doubling roughly every three years [18]. This trajectory mirrors the cost reduction achieved during the initial years of oil exploitation a century ago. Forecasts from the Danish Energy Agency suggest a further 50% cost reduction by 2020, while the EU Commission estimates a minimum 30% reduction in wind power energy costs between 1998 and 2010 [18].

I.14 Types of wind turbines

There are two primary categories of wind turbines: those with rotors rotating around a horizontal axis and those with rotors rotating around a vertical axis. Vertical-axis wind turbines (VAWTs) can be further classified into two main groups: those utilizing aerodynamic drag and those utilizing lift to extract power from the wind. The vertical axis of rotation allows for the placement of the generator and drive train at ground level. However, VAWTs face challenges such as difficulty in controlling power output through blade pitching, lack of self-starting capability, and low tip-speed ratio.

On the other hand, horizontal-axis wind turbines (HAWTs) are conventional and unlike VAWTs, are not omnidirectional. In HAWTs, the generator directly converts wind energy extracted by the rotor. Control over rotor speed and power output can be achieved by pitching the rotor blades along their longitudinal axis, facilitated by mechanical or electronic blade pitch control mechanisms. HAWTs offer advantages such as blade pitching providing protection against extreme wind conditions and over speed, and the ability to shape rotor blades to optimize turbine efficiency by maximizing aerodynamic lift.

The main components of HAWTs include the blades, hub, transmission system, gearbox, generator, and yaw and pitch control systems. Blades are crucial to the turbine's operation, with three-bladed designs being most common in modern turbines. These blades are attached to the central hub, generating an imaginary surface known as the swept area as the rotor rotates.

I.15 Archimedean Spiral-Type Wind Turbine

The Archimedes spiral wind turbine, a novel concept within the realm of horizontal-axis wind turbines (HAWTs), is engineered based on the principles of the Archimedes spiral. Diverging from traditional HAWTs that rely solely on lift force to harness wind energy, the Archimedes spiral wind turbine utilizes both lift and drag forces. This innovative approach allows the turbine to tap into the kinetic energy inherent in wind currents.

The unique structure of the Archimedes spiral wind turbine gives rise to distinct aerodynamic characteristics, particularly beneficial for small-scale wind turbines. These advantages are particularly evident in various scenarios, such as urban environments, where the turbine operates efficiently at low wind speeds. Notably, the turbine automatically aligns with changing wind directions in urban settings, owing to passive yaw control facilitated by drag force. Additionally, the turbine generates minimal noise due to its relatively low rotational speed.

However, it is worth noting that the Archimedes wind turbine exhibits a drawback in the form of high thrust force compared to conventional propeller-type HAWTs [19].

I.16 the Archimedean Spiral

The Archimedean spiral derives its name from the ancient Greek mathematician Archimedes, dating back to the 3rd century BC. It represents the path traced by a point moving away from a fixed point at a constant speed along a line that rotates with a consistent angular velocity over time. In polar coordinates (r, θ), its equation is typically expressed as $r = a + b\,\theta^{(1/c)}$. Adjusting the parameter "a" results in rotational changes to the spiral, while "b" determines the spacing between consecutive turns. The standard Archimedean spiral is achieved when the parameter "c" equals 1.

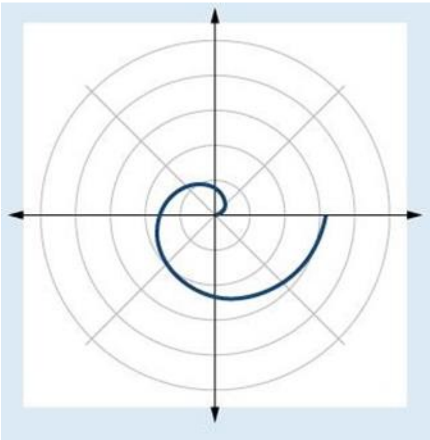

FigureI.12 Archimedean Spiraling a graph [19].

I.17 Archimedes Rotor

The Archimedes rotor combines features of both resistance and lift-type turbines. Its resistance characteristics include flat blade sheets, tolerance to substantial margin of error, minimal noise production, and lightweight construction. Additionally, the turbine rotor can operate efficiently with a tip speed ratio exceeding 1, showcasing characteristics akin to lift-type rotors.

Designed based on the principles of the Archimedean Spiral, the rotor features a spiral-shaped blade configuration that facilitates thorough airflow within the blades, enabling utilization of both drag and lift forces. Comprising three blades interconnected at 120-degree intervals, each blade exhibits an asymmetric arrangement around the shaft and adopts a shape resembling a triangular pyramid. The Archimedes-shaped spiral wind blade demonstrates notably higher rotor efficiency compared to other blade designs, such as the Savonius-type rotor, particularly within the lower tip speed ratio range.

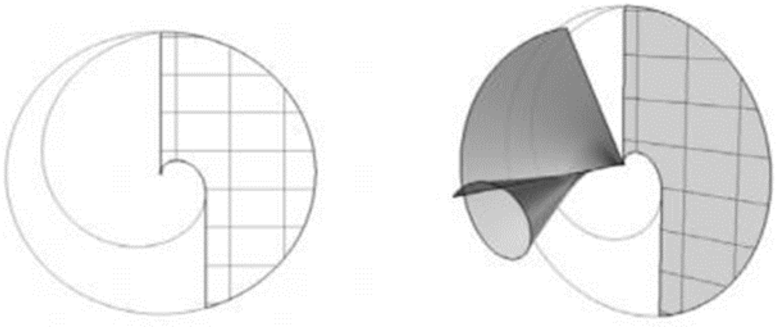

Figure I.13: The used flat plane and extended spatial figure for Archimedean Spiral blade [19]

The Archimedes spiral wind turbine, classified as a horizontal-axis wind turbine (HAWT), presents a notable departure from traditional HAWT designs. The spiral configuration introduced by Archimedes initially offered improved methods for measuring a circle's circumference and area. However, its utility was surpassed when Archimedes developed a more precise value for π, facilitating a simpler approach to measuring circle areas.

In contrast to conventional HAWT models, which primarily rely on lift force to harness wind energy, the Archimedes spiral small wind turbine predominantly utilizes drag force as its primary mechanism for power extraction.

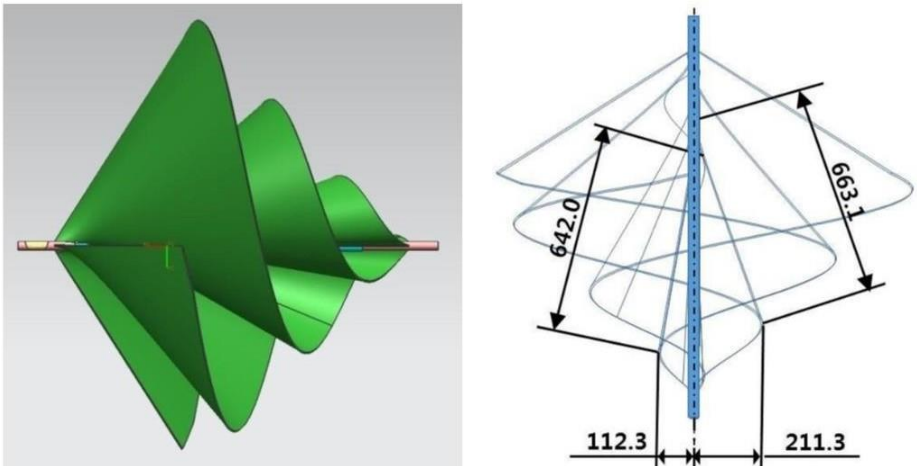

Figure I.14 GeometryofArchimedesWindTurbineBlade [19]

In March 2007, testing conducted in Delft demonstrated an efficiency of approximately 10%. Subsequently, an enhanced model was tested in 2009 at the Peutz Wind Research Center, reaching a breaking point at 21m/s wind speed. Modifications were made to reduce the number of revolutions along the rotor axis from pi to one, resulting in an efficiency increase to about 15%. In 2012, a comprehensive study commenced at Pusan Korea University, with CFD analysis confirming earlier calculations and indicating a theoretical efficiency of 25%. Over the following two years, rotor efficiency remarkably rose to an astonishing 52% [19].

I.18 Turbine Aerodynamics

I.18.1Tip Speed Ratio

The tip speed ratio, a crucial parameter in wind turbine design, represents the ratio of the blade tip speed to the wind speed. This ratio plays a pivotal role in determining the turbine's efficiency. Its mathematical representation is illustrated in the equation below:

Definition of tip speed ratio,

$$\lambda = \frac{\omega \times R}{V0} \qquad (1)$$

ω represents the angular velocity of the wind turbine rotor, R signifies the radius of the rotor, and V_0 denotes the wind speed. An increased tip speed ratio correlates with elevated noise levels and necessitates sturdier blades to withstand the substantial centrifugal force. The connection between rotational speed and tip speed ratio is depicted in the equation below:

$$\lambda = \frac{2MNR}{60V0} \qquad (2)$$

In this equation, N represents the rotational speed of the rotor, R stands for the rotor radius, and V_0 denotes the wind speed. Consequently, a reciprocal correlation between the rotational speed and the blade span can furnish the necessary velocity. Given a constant tip speed ratio, a blade with a larger span operates at a lower rotational speed [16].

I.18.2Power and Torque

In practice, a wind turbine is unable to extract the entirety of the wind power as it passes through the rotor. Consequently, a portion of the wind's kinetic energy is transferred to the rotor while the remaining energy exits the rotor. As a result, the proportion of wind energy converted into mechanical power by the rotor is quantified as the efficiency, commonly referred to as the power coefficient, Cp.

Aerodynamic Efficiency,

Where,

T=Torque

ω=Angular velocity

A = Swept area of the blade V=Wind velocity

I.18.3 Betz limit

Efficiency is determined by the ratio of the power coefficient (Cp) to the Betz limit, which is defined as 16/27, approximately equal to 0.593. This limit, established by German physicist Albert Betz in 1919, represents the maximum achievable power coefficient for a wind turbine that converts kinetic energy into mechanical energy. Thus, efficiency can be calculated using the following formula:
Efficiency=Cp×Betz Limit

Where Cp represents the power coefficient.

I.19 Computational Fluid Dynamics (CFD)

Computational Fluid Dynamics (CFD) is a computational technique utilized for forecasting fluid flow, heat transfer, and chemical reactions within intricate systems. Widely employed across industrial and non-industrial sectors, CFD offers expedited and cost-effective means for modeling designs. To conduct fluid analysis using CFD, it is essential to acquire the mathematical equations that elucidate the fluid flow behavior [20].

I.19.1 Principle the ories relevant

In Computational Fluid Dynamics (CFD) modeling, regardless of the specific software used, the core simulation processes remain consistent. The initial step involves establishing governing equations, with mass, momentum, and energy conservation equations forming the fundamental basis. Subsequently, boundary conditions are determined to accommodate different flow scenarios, followed by the creation of a mesh. Meshing serves to discretize equations and boundary conditions into a cohesive grid structure, where the cell serves as the basic element. In two-dimensional unstructured grids, triangular and quadrilateral cells are common, while rectangular cells are prevalent in structured grids. In three-dimensional simulations, tetrahedral and pentahedral cells are typical in unstructured grids, whereas hexahedral cells are utilized in structured grids. Mesh quality is imperative for obtaining physically accurate solutions, contingent upon the expertise of the simulation engineer. Efficient mesh creation is essential, as a higher node count within the mesh results in increased computational time. Three numerical methods—Finite Difference Method (FDM), Finite Element Method (FEM), and Finite Volume Method (FVM)—are utilized to discretize equations. FVM, widely employed in CFD software such as Fluent, Ansys Design Modler, PHOENICS, and STAR-CD, offers advantages over FDM and FEM due to its compatibility with unstructured meshes and adaptability to various geometries [16].

I.19.2 Turbulent models

In CFD software, wind turbines undergo simulation within turbulent flows. There are three distinct methods for simulating turbulent flows under Indirect Numerical Simulation:

Large Eddy Simulation (LES), Reynolds-averaged Navier-Stokes (RANS), and Detached Eddy Simulation (DES). The Reynolds-averaged Navier-Stokes (RANS) equation is defined as follows:

$$\frac{\mathbf{d\mu i}}{\mathbf{dt}} = \frac{\partial \mathbf{P}}{\partial \mathbf{Xi}} + \frac{\partial}{\partial \mathbf{Xi}}\left[\mu\left(\frac{\partial \mu i}{\partial xj} + \frac{\partial \mathbf{\mu i}}{\partial \mathbf{xi}}\right) - \overline{\rho\mu' \jmath \mu' \imath}\right] \tag{4}$$

On the left-hand side of the equation, the description pertains to the alteration in the mean momentum of a fluid element. Conversely, the right-hand side of the equation represents the postulation of mean body force and stress divergence. The term $\overline{\rho\mu' \jmath \mu' \imath}$ denotes an unidentified quantity known as Reynolds stresses.

I.19.3Solution Methods

- Standard k−ε model: Known for its stability and precision in turbulent flows with high Reynolds numbers, this model may not be suitable for simulations involving rotational effects.
- RNG k−ε model: Particularly effective for low Reynolds number flows, this model enhances simulation accuracy in rapidly strained flows by accounting for rotational effects.
- Realizable k−ε model: This model offers greater accuracy in predicting the speed rate of both planar and round jets. However, it may produce non-physical turbulent viscosities when simulating models that include both rotating and stationary fluid zones.
- Standard k-ω model: Incorporating low-Reynolds-number effects, compressibility, and shear flow spreading, this model demonstrates good agreement with measurements. It may encounter challenges in scenarios involving far wake, mixing layers, and various jet configurations.
- Shear-stress transport (SST) k-ω model: Combining the advantages of the standard k-ω model's accuracy in the near-wall region and the precision of the k−ε model in the far field region, this model is considered more accurate and reliable for a wider range of flows.
- Reynolds stress model: Unlike the eddy-viscosity hypothesis used in k−ε and k-ω models, the Reynolds stress model (RSM) directly calculates Reynolds stresses. While theoretically more accurate, this model requires the solution of additional transport equations, making it computationally more demanding.

I.20 Conclusion

In this chapter, we provided an overview of wind energy, covering both vertical and horizontal axis wind turbines. While discussing the operations of horizontal axis wind turbines in more detail, we also highlighted various aspects of wind power concerning the environment, noise, visual impact, and other relevant factors.

Chapter II Research methodology

II.1. Introduction:

This chapter outlines the methodology adopted for the CFD study of the mobile Archimedes wind turbine using Ansys software. Initially, various turbine designs, including blades and shaft configurations, are subjected to analysis within the simulation software, creating a virtual environment. Aerodynamic properties are assessed under a single wind speed to identify the optimal geometry model. Subsequently, the model's characteristics are re-evaluated. Following this, the model is fabricated and tested, with the results compared against those obtained from the CFD simulations. Finally, a theoretically feasible prototype is designed for power harnessing purposes.

II.2. configuration:

In this investigation, we consider an average wind speed of 10 m/s, equivalent to 36 km/h. It's worth noting that wind turbines need to rotate effectively even at lower wind speeds. Typically, wind turbine design and sizing are predicated on a minimum speed of 5 m/s, which equals 18 km/h. **Figure 2.1** illustrates the design of the Archimedes wind turbine under study, resembling the repetitive shape of a nautilus shell.

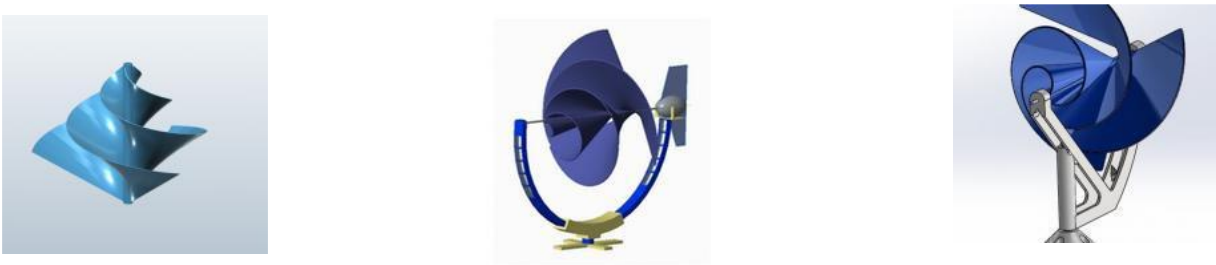

Figure II.1 Configuration of an Archimedes wind turbine[19]

II.3. Software description:

The turbine geometry was designed using SOLIDWORKS 21 to achieve the desired shape. SOLIDWORKS facilitated the design process by providing accurate guidance and ease of use.

For the CFD simulation, the Academic multipurpose CFD solver ANSYS FLUENT was employed. The solver is tailored to adhere to the Reynolds Averaged Navier Stokes Equation and employs the Finite Volume Method for solving the governing equations. To accurately predict flow separation, the k-ω Shear Stress Transport (SST) turbulence model was selected.

Mesh generation was accomplished using ANSYS MESHING.

II.4. Design Parameters estimation:

To establish the simulation system for the turbine, several parameters are employed to define its virtual characteristics. These parameters are broadly categorized into two types: Input parameters and Variable parameters. Additionally, geometric constraints are considered.

The Input parameters consist of:
1. Wind Velocity
2. Angular Velocity
The Variable parameters include:
1. Pitch
2. Opening Angle

Geometric constraints are also accounted for, such as:
1. Blade Diameter

II.4.1. Wind Velocity

The wind velocity, known as the input wind, encompasses a range of speeds. However, for consistency, an average wind velocity, denoted as Vavg, is set at 3.5 m/s. This value remains constant across different simulations of turbine geometries. Once the optimal geometry is determined, simulations are conducted across a range of wind speeds up to 12m/s.

II.4.2. Angular Velocity

The angular velocity represents the rotational speed of the turbine. Since the optimal rotational velocity for maximum efficiency is not predetermined, a range of rotational velocities is considered for analysis rather than a single fixed value. This approach allows for a comprehensive examination of the turbine's performance across different rotational speeds.

II.4.3. Pitch of the blade

The pitch of the wind turbine blade is a crucial factor in turbine design, as it regulates the turbine's rotational speed and adjusts it in response to changes in wind speed. Determining the appropriate pitch is critical for optimizing power generation and minimizing turbine fatigue. In the simulation process, the pitch is adjusted and analyzed to understand its impact on turbine performance.

II.4.4. Opening angle

The opening angle of the turbine influences the airflow within the blades and their surroundings, as well as the formation of tip vortices at the blade ends. Additionally, changes in the opening angle affect the pressure distribution along the turbine blades. In the simulation process, the opening angle is adjusted and analyzed to assess its impact on turbine performance.

II.5 Aerodynamic Analysis of the Turbine

II.5.1. Modelling of Geometry

The turbine comprises a single shaft and three blades, all with an equal diameter. Initially, the turbine design is created using SOLIDWORKS 21, with the blades set to a diameter of 150 mm. A helix with variable pitch, available in the software, is utilized to impart the necessary curvature to the blades, with the specified variable pitch input accordingly. A total of 12 different geometries with various dimensions are constructed.

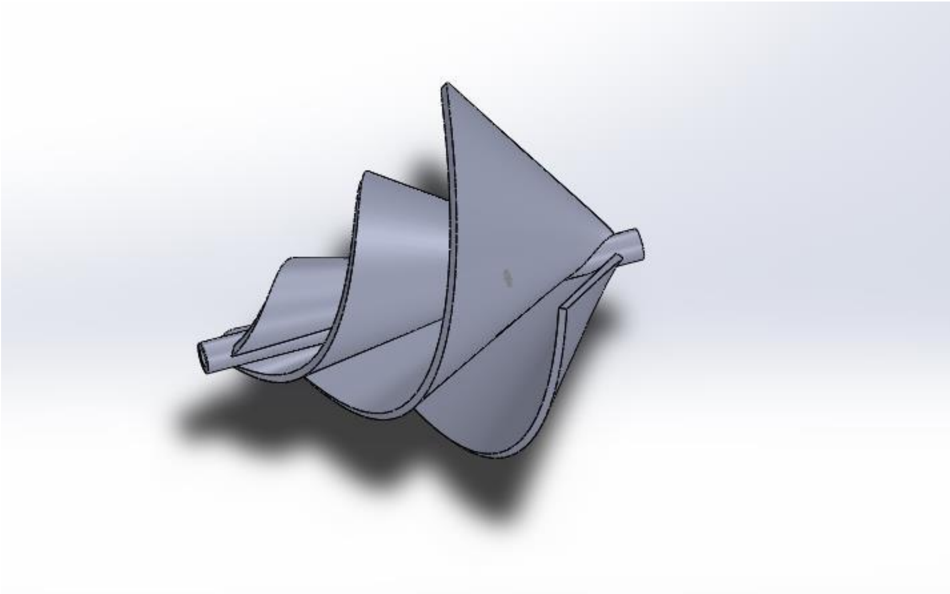

Figure II.2 Model of turbine rotor with pitch at 112.5 mm[19]

II.5.2. Grid Generation (Mesh Geometry)

The geometry is imported into ANSYS MESHING 16, where a single domain is generated to encompass the turbine. An O-grid is created around the turbine geometry to facilitate dense meshing and proper inflation. The node distribution varies based on the required mesh density. Wall distances for the first edge near the wall are determined using parameters such as reference length, flow velocity, density, and viscosity.

$$Y^{+}=\frac{\mu * y}{v} \qquad (5)$$

The equation for Y^{+} is as follows:

$Y^{+} = \frac{\mu * y}{v}$

Where:

- μ is the friction velocity at the nearest wall,
- y is the distance to the nearest wall,
- v is the local kinematic viscosity of the fluid.

The non-dimensional wall distance for a wall-bounded flow is represented by Y^{+}.

The wall distance values of the model range from 0.2 mm to 0.32 mm, depending on the increase in velocity. These values were obtained using the Y-Plus Distance Estimation tool from the online source www.cfdonlinetools.com. The tool requires input parameters such as free-stream velocity, fluid density, dynamic viscosity, boundary layer length, and the desired Y^{+}. Value, which in this case is 4 for the SST Model. This input helps estimate the approximate Reynolds number and wall distance.

Table II.1: Basic Paramètres

S.N.	Paramètres	Value
1	Free Stream Vélocité	3.5 m/s
2	Densité	1.225 kg/m3
3	Dynamics Viscosité	1.875*10-5 kg/ms
4	Boundary Layer length	0.162 m

II.6. Fluent Simulation

The mesh generated is imported into Fluent for further analysis. In the setup process, fluid properties and the turbulence model are selected, and boundary conditions for flow velocity and pressure values are defined. Additionally, the cell conditions are modified to fluid within ANSYS MESHING. After initialization, the calculation process begins.

II.7. Fluent setup parameters

To ensure a consistent comparison across different geometries, the Fluent setup parameters remain constant for each trial. The selected models are as follows:

- Viscous model: SST k-ω with all parameters set to default values.
- Material: Air (Assumed to be incompressible).
- Viscosity: Maintained as constant.
- Ambient pressure and temperature: Standard atmospheric conditions (101325 Pa and 288.15K).

II.8. geometry and design

Using SolidWorks-21 CAD software, the wind turbine design comprises two primary components:

- A central cylinder, 1.5 meters in length, formed by extruding a circle with a diameter of 2.5 centimeters.
- A boundary surface, 2.5 millimeters thick, shaped as a 60-degree outward conical spiral propeller with a pitch of 0.750 meters, completing a single revolution. This surface is replicated three times around the central cylinder, evenly spaced at 120-degree intervals.

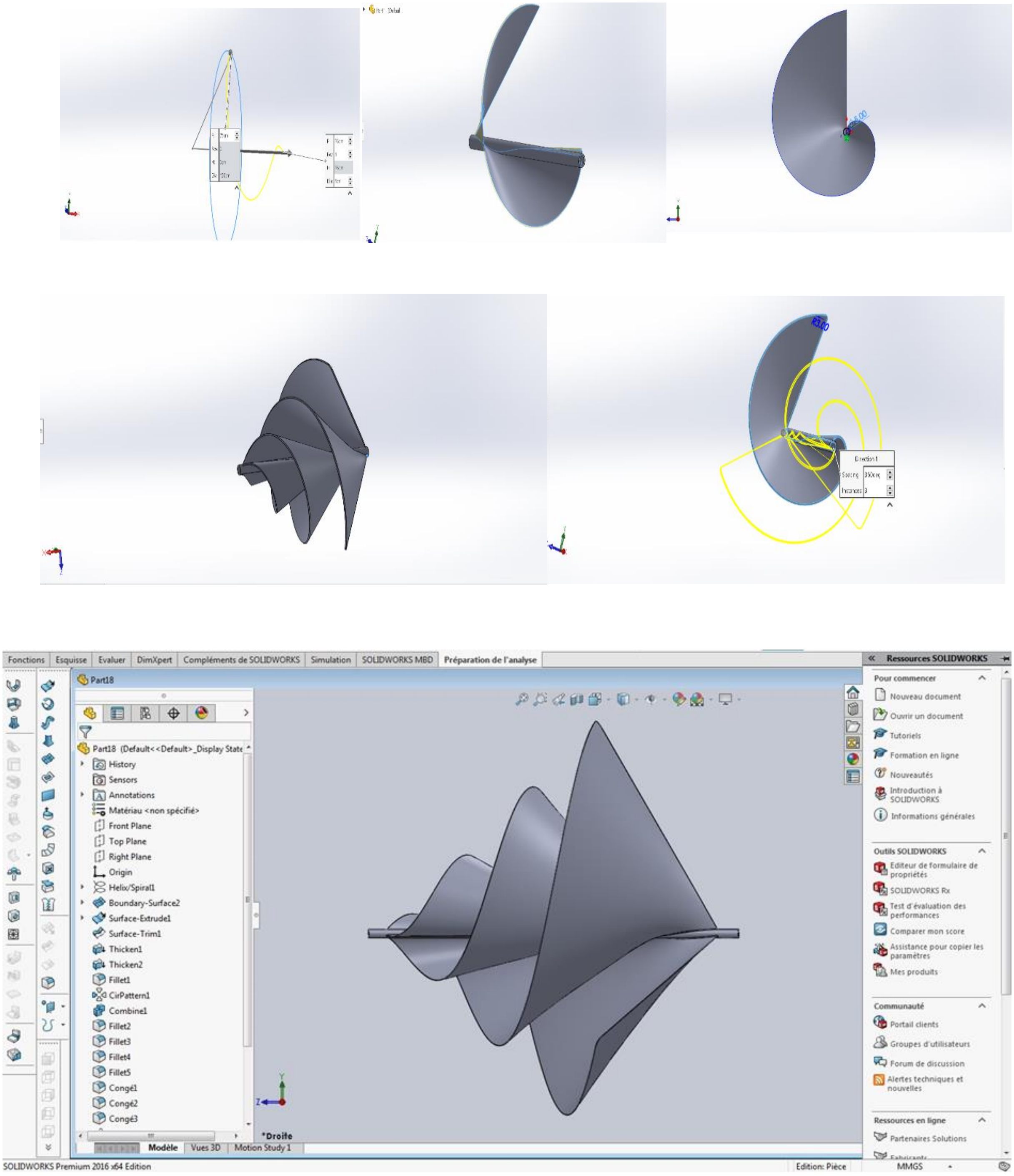

Figure II.3 the main design stages of the Archimedes wind turbine assisted by SolidWorks-21

II.9. Conclusion

By combining these strategies and investing time in learning and practicing, we can strengthen our expertise in using Solid works 21 for turbine design and achieve more accurate, more realistic results.

Chapter III

Design and simulation

III.1. Introduction

Simulation involves utilizing a computer or network to replicate a real and intricate physical phenomenon. Scientific numerical simulations rely on applying theoretical models to examine the operation and characteristics of a modeled system, as well as to forecast its progression. This process is often referred to as numerical calculation. Graphical interfaces enable the visualization of computational outcomes through synthetic images. "Digital" refers to the execution of computer programs.

III.2. Presentation of simulation software:

III.2.1SolidWorks software:

SolidWorks is a proprietary 3D computer-aided design (CAD) software designed for Windows operating systems. It functions as a 3D modeler employing parametric design principles. The software produces three types of files corresponding to three fundamental concepts: the part, the assembly, and the drawing. These files are interrelated, meaning that any alteration made at any level is automatically updated in all associated files.

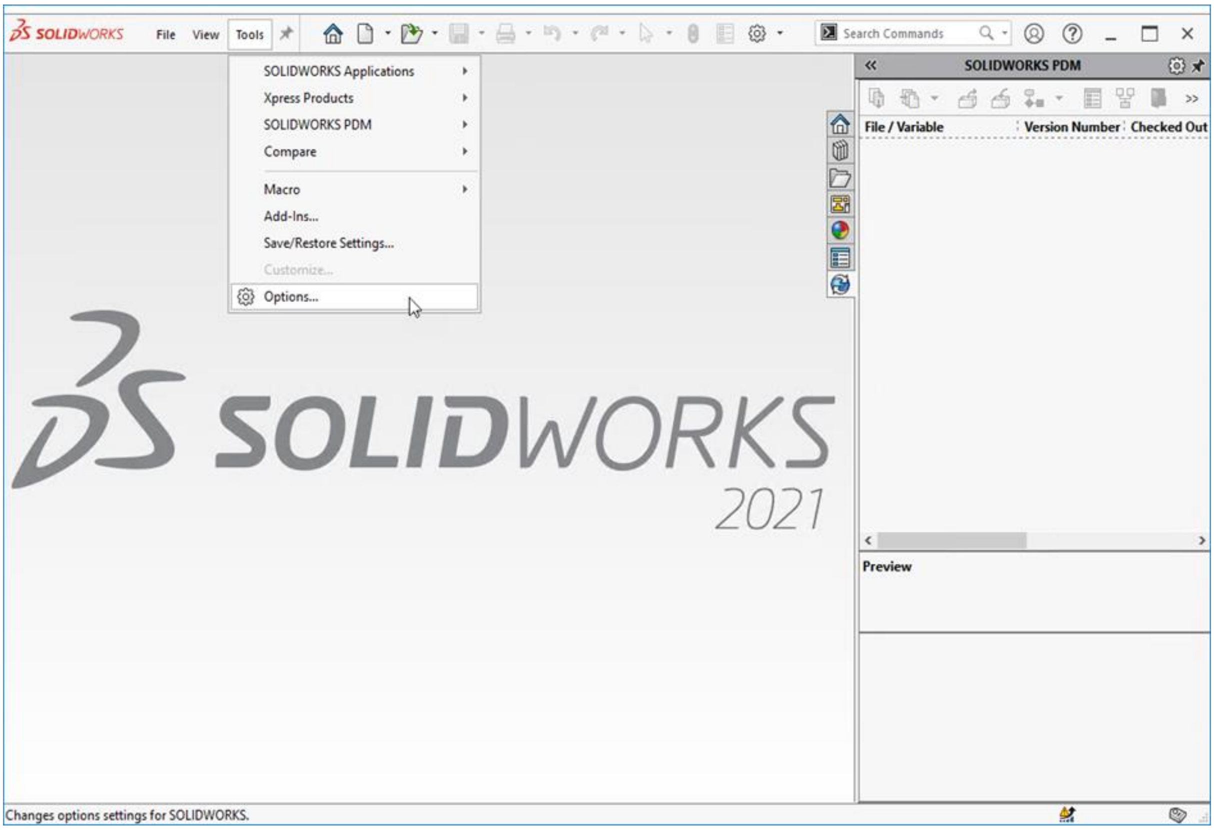

Figure III.1: Interface solidworks21.

III.3 CFD simulation

III.3.1. Design

In this study, Ansys Design Modeler R22.2 software will be utilized. However, since Ansys Design Modeler cannot directly read SolidWorks files with the .SLDPRT extension, it is necessary to convert them to an IGES file format (.IGS). IGES, which stands for Initial Graphics Exchange Specification, is a graphics data export format that is compatible with various CAD software. This export format offers a high degree of universality, especially in the realm of surface and wireframe-oriented 3D CAD. **Figure III.2** illustrates the geometry of the open wind turbine in the Ansys Modeler design.

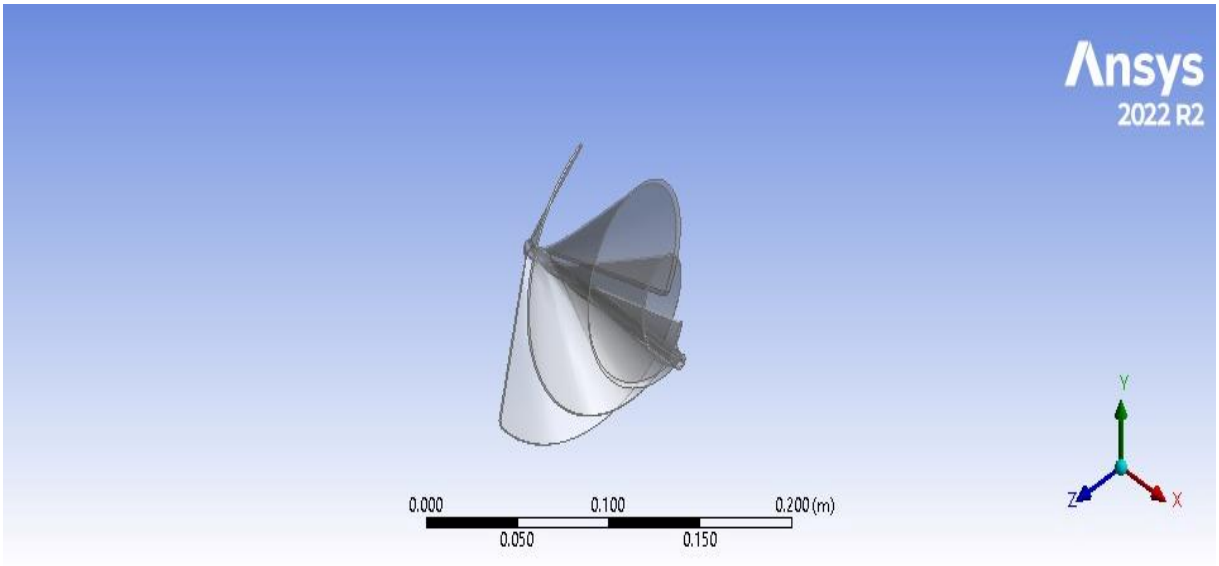

Figure III.2 The Archimedes wind turbine in Ansys Design Modler.

So far, we've only modeled the solid representation of the wind turbine. Since our objective is to conduct a CFD study around this wind turbine, we need to define a domain that encompasses our Archimedean wind turbine. The Design Modeler offers a useful function called "Encompass," which enables us to select the shape of the domain and its dimensions (such as cylinder or box) to enclose the device under study. We opted for a rectangular box placed at a sufficient distance to minimize aerodynamic disturbances. Given that the wind turbine is mobile, it needs to be enclosed within a cylinder. We have renamed the box as "Fluid" and the wind turbine as "Solid," as depicted in **Figure III.3.**

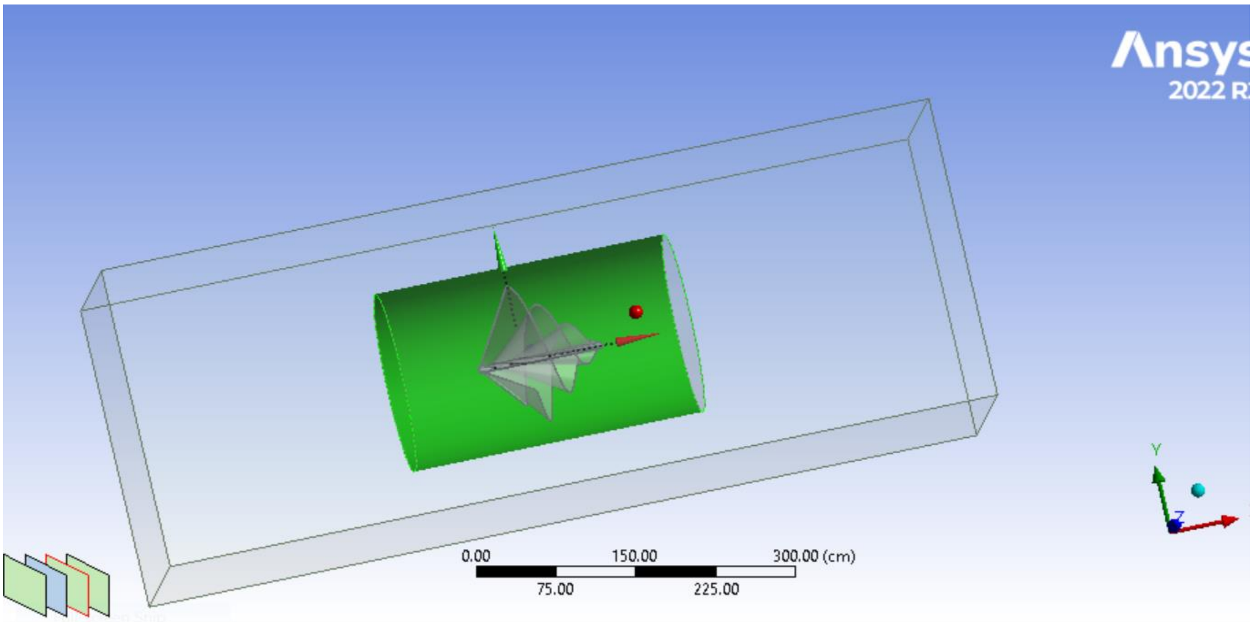

Figure III.3 the Archimède wind turbine encompassed in two areas: cylinder and parallelepiped.

III.3.2. Mesh Generation

The mesh is created using the Ansys Mesh module, which offers both automatic generation and user-controlled options. Users can apply various functions like refinement, sizing, pinching, and inflation according to specific requirements. In this study, the mesh generation is automated with the inflation option activated. After generation, the mesh consists of 1,840,521 elements and 333,100 nodes. Figure 3.4 displays the generated mesh by Fluent-CFD. Additionally, **Figure III.4** B provides a close-up view of the mesh around the AWM wind turbine..

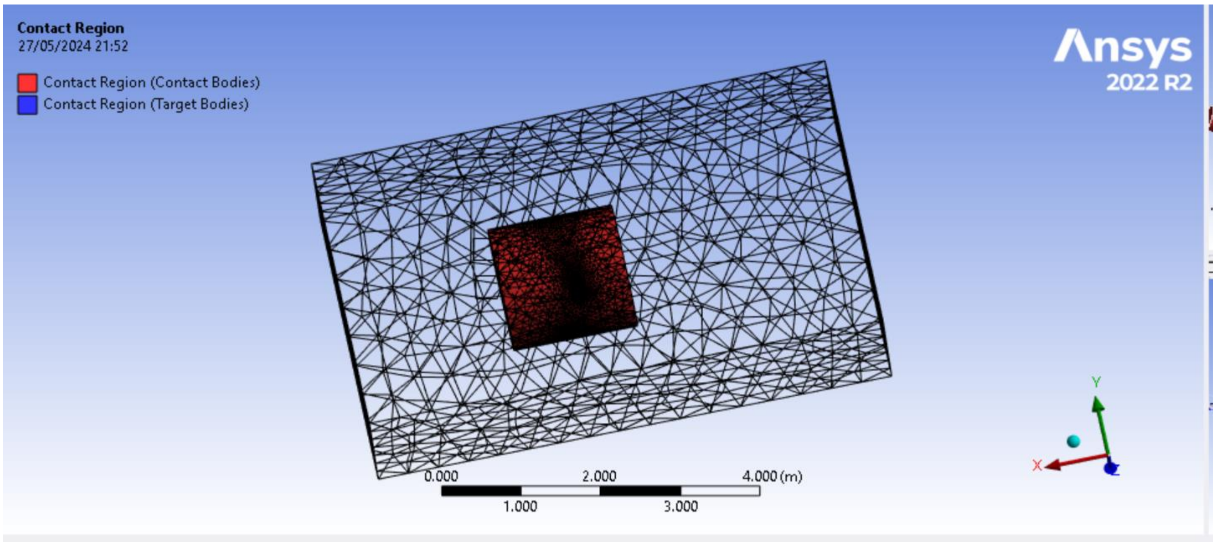

Figure III.4.A Mesh generated around the Archimedes wind turbine enclosed in a parallelepiped and cylinder.

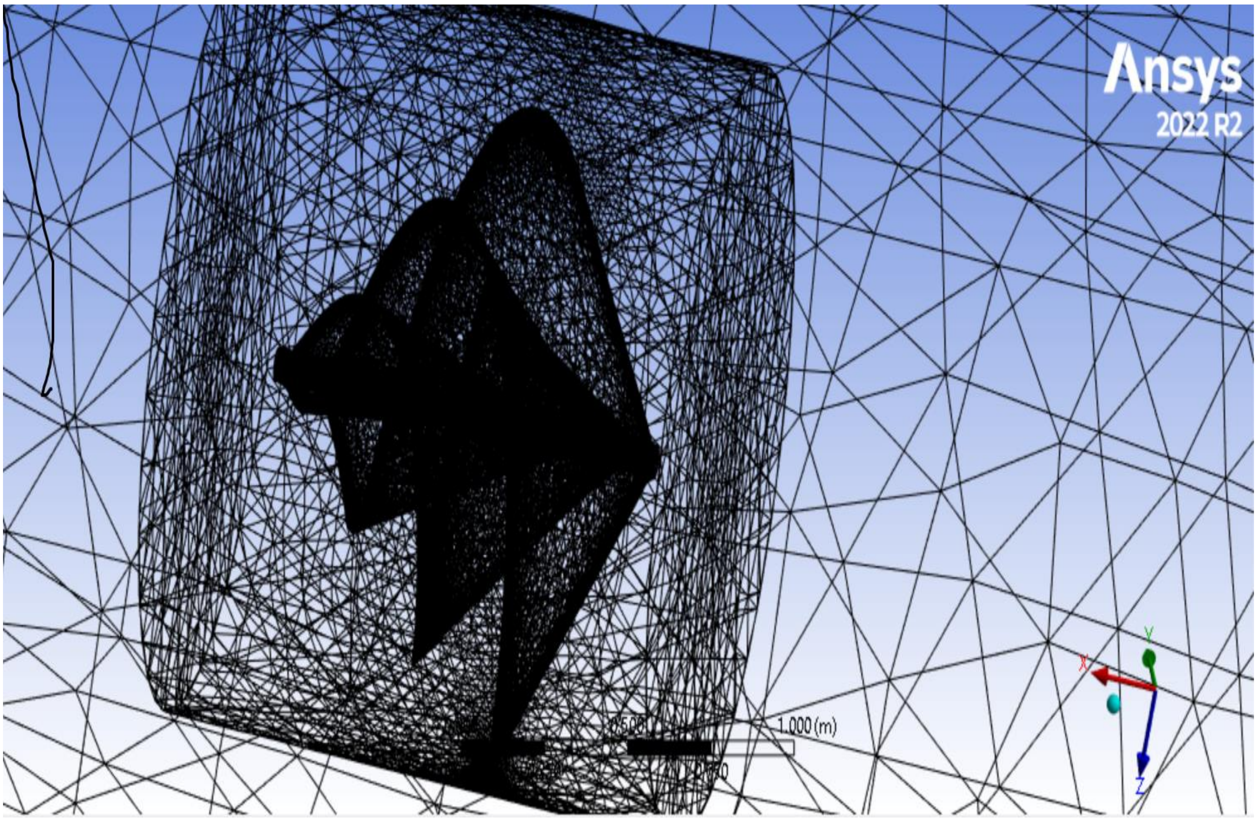

Figure III.5.BMesh zoom generated around the wind turbine.

Choice of thickness 1ermesh

The inflation option was employed to capture the boundary layer, aligning with the requirements of the K-Epsilon turbulence model, which mandates a Y+ ranging from 20 to 50. Utilizing an online resource [21], the thickness of the initial mesh layer e was determined, considering parameters such as air speed, dynamic viscosity, density, reference length, and targeting a Y+ value of 30. Seven layers were selected with a growth rate set at 1.2, as illustrated in **Figure III.5**.

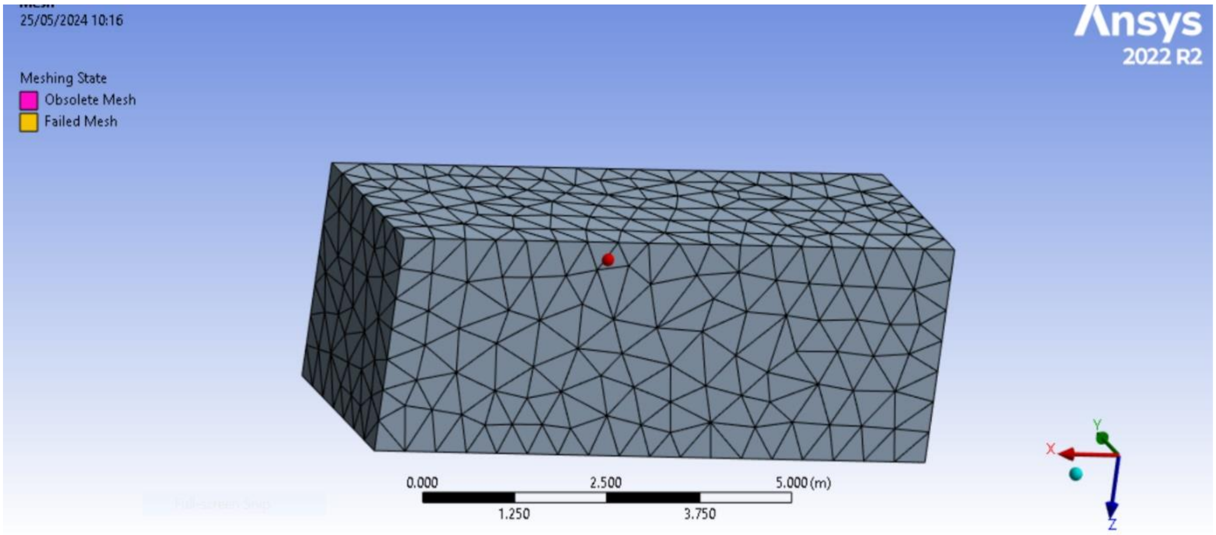

Figure III.6: Boundary layer capture**.**

III.3.3 Establishment of boundary conditions

The fluid considered is air at 25°C, flowing under steady-state isothermal conditions within a continuous medium at a reference pressure of 1 atm, and subjected to non-buoyancy conditions. The turbulence model selected for the simulation is the scalable k-epsilon model. Boundary conditions are specified in the Ansys Design Modler -Pre module, as depicted in **Figure III.6.**

1) Fluid Domain (parallel piped box):

Entry requirement: We established a constant velocity of 15 m/s perpendicular to the air inlet face of the cube. The flow is subsonic, with an inlet turbulence intensity of 5%.

Exit condition: We designated the OUTLET condition with a relative pressure of "0 pascal" with a flow direction perpendicular to the outlet face.

2) Exterior wall condition: The free-slip condition is imposed on the outer walls of the computational domain to mitigate the impact of wind on the wind turbine, ensuring that the flow remains entirely slipper on these surfaces.

3) Rotation domain (AWM): The no-slip condition is enforced on the walls of the wind turbine to accurately capture the boundary layer. Additionally, the wind turbine is pre-designated as mobile, rotating at a speed of -6 radians per second, while considering heat transfer effects.

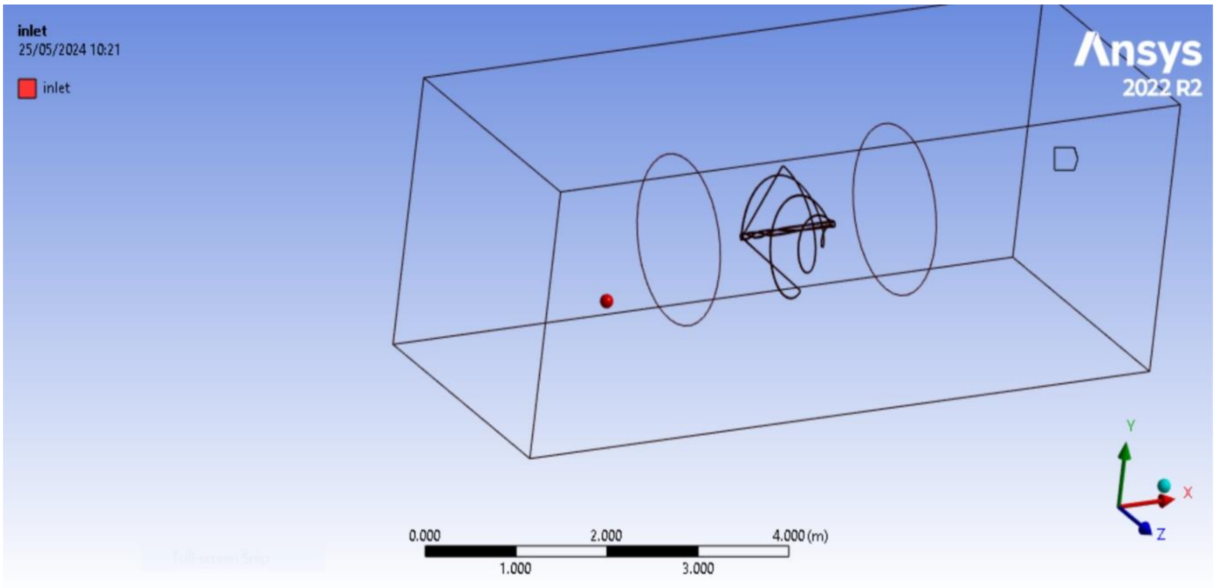

Figure III.7 Boundary Conditions in Ansys Design Modler -Pre.

III.4. Boundary conditions

The turbine maintains a constant speed of 3.5 meters per second, operating at sea level where the fluid is subjected to normal atmospheric pressure, resulting in a gauge pressure of 0. The Reynolds number was determined as Re = 4.937 × 104 using the following equation:

$$Re = \frac{\rho V l}{\mu} \quad (6)$$

Where,

ρ = 1.225 kg/m3,

μ = 1.875 ×10-5 kg/m-s,

l = reference length = 162 mm

Different models were used for the same boundary conditions but with varying tip-speed ratios

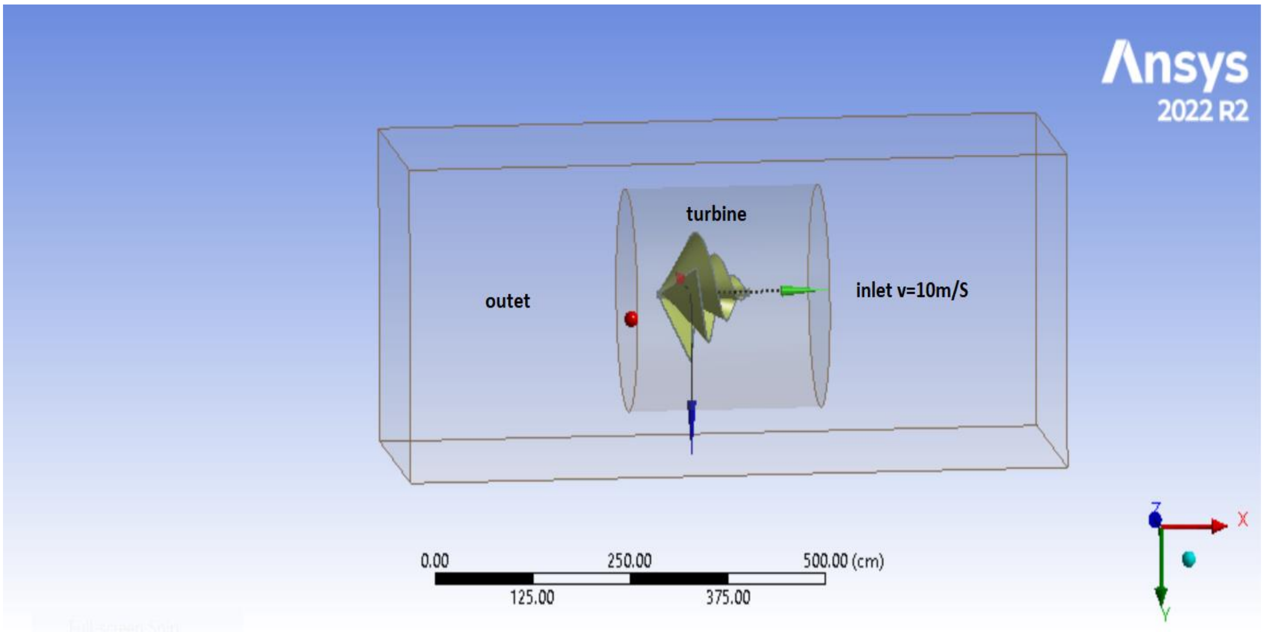

Figure III.8: Turbine domain setup in ANSYS DM

Table III.1: Table representing Different Boundary Conditions

N	Zone	Boundary Type	Operating Condition
1	Inlet, top and bottom	Velocity Inlet	10 m/s (x-direction)
2	Interior-domain	Interior	0 Pascal (Gauge pressure)
3	Outlet	Pressure Outlet	0 Pascal (Gauge pressure)
4	Turbine	Wall (ABS Plastic)	-

Velocity inlet the boundary condition is established to specify the velocity magnitude and direction of the incompressible fluid flow. This ensures that the flow is provided at various inclinations from the global axes.

Pressure outlet Boundary conditions necessitate the specification of a static (gauge) pressure at the outlet boundary.

Reference Values The parameters to be set include area, density, enthalpy, length, pressure, temperature, velocity, dynamic viscosity, and ratio of specific heats. During the analysis, all parameters are initially set to default values when computing from the inlet..

Solver

Second order discretization upwind is used to solve the problem with **a pressure based solver.**

Each boundary condition is initialized with a flow velocity value, and then iterations are executed. Among the available solver algorithms in ANSYS FLUENT, a **coupled algorithm** is chosen for the problem over a segregated one.

III.5. Determination of Best Model

Steady-state simulations are conducted for various geometries, with each geometry analyzed across a range of tip speed ratios to identify the tip speed ratio that yields the maximum power coefficient. Different geometries exhibit varying optimal tip-speed ratios for achieving maximum power coefficients.

In this analysis, the boundary conditions are as follows:

- Inlet wind speeds ranging from 1 to 15 m/s at intervals of 2 m/s
- Rotor angular speeds ranging from 100 to 500 rpm at intervals of 100 rpm
- Outlet condition set to atmospheric pressure
- Wall conditions set to no-slip

Initially, a 3D CFD analysis is performed with wind speeds ranging from 1 to 15 m/s and rotor speeds ranging from 100 to 500 rpm. The wind speed is assumed to be uniform.

Table III.2- Data obtained from CFD analysis

N	Wind speed (ms^{-1})	Torque(AWT) N-m
1	1	0.42
2	3	3.24
3	5	7.95
4	7	16.10
5	9	25.98
6	11	38.93
7	13	55.06
8	15	72.87

The results obtained from the comparison between the Archimedes airfoil wind turbine (AWT) and the Archimedes spiral wind turbine (ASWT) are presented in Table III.2, extracted from the CFD Fluent analysis. Figure III.8 illustrates the torque of the AWT at various wind speeds. The results indicate a torque increase ranging from approximately 10% to 15% at low speeds and exceeding 15% at moderate speeds. The flow direction is from left to right, influenced by the spiral and airfoil shape of the turbine blades, resulting in increased velocity from the leading edge towards the inner side of the blade, thus facilitating fluid flow.

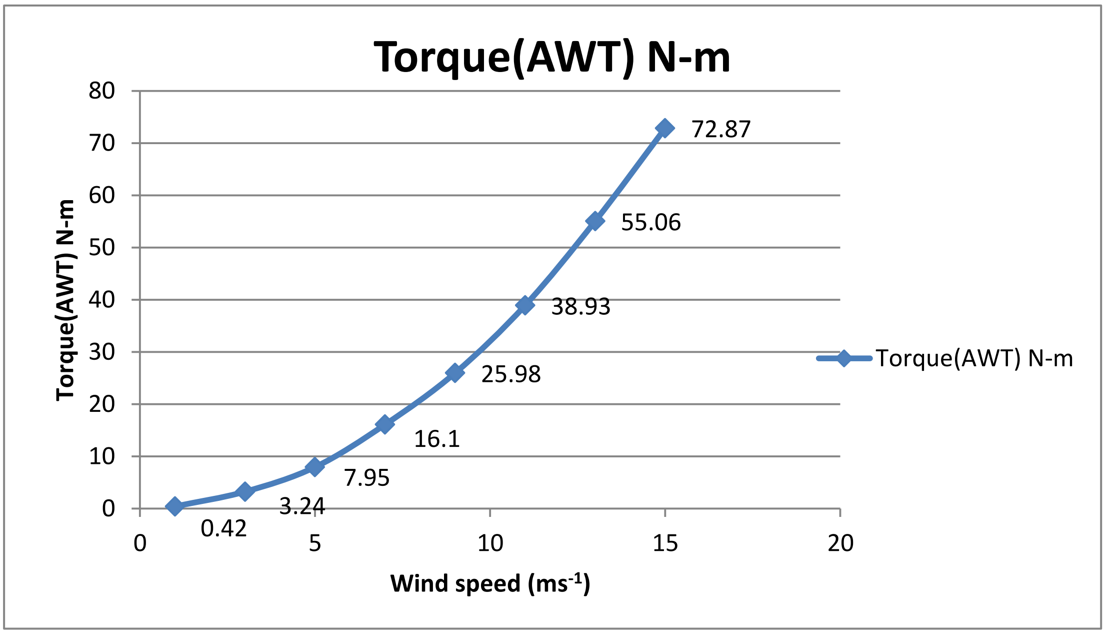

Figure III.9. Torque comparison

Accelerates of the blade and highest velocities have detected at the end tip of the blade as shown in fig III.9

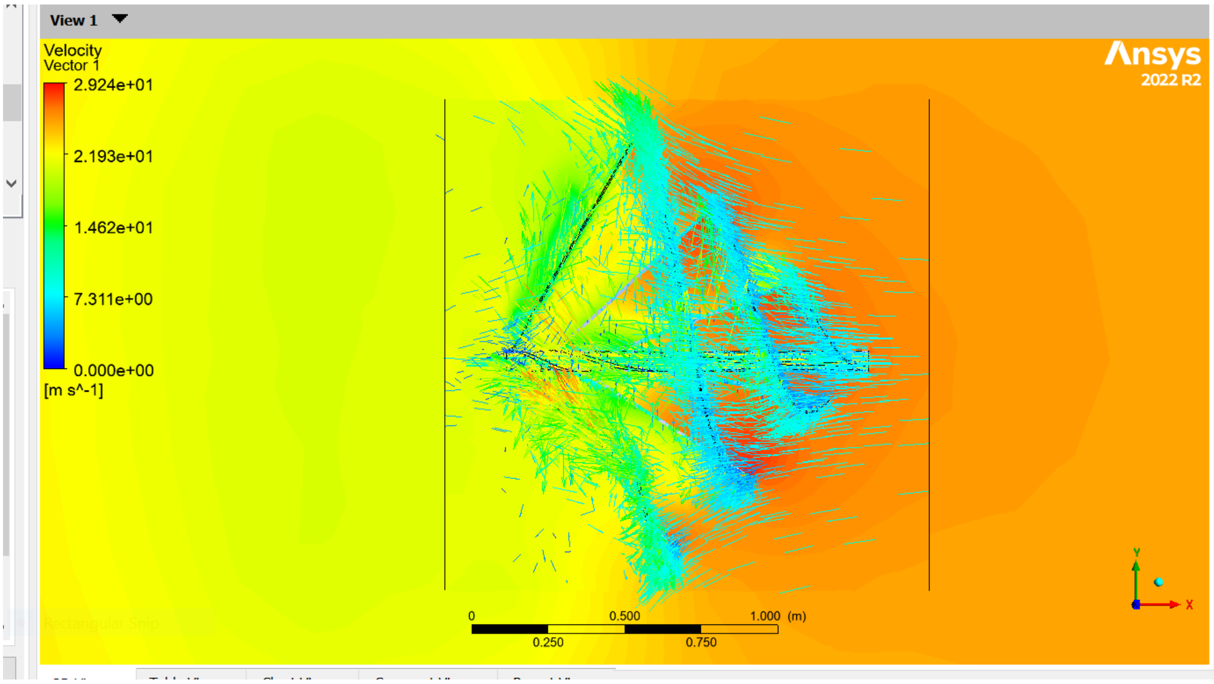

Figure III.10. Direction of flow filed over turbine blade

Table III.3: Simulation data for different tip speed ratios at pitch = 0.25R

λ	**ω (rad/s)**	**T (× 10^{-3} N-m)**	**P (W)**	**C_p**
1	45.6666	1.029	0.03850	0.10352
1.25	57.3333	0.764	0.04042	0.10766
1.5	70	0.625	0.04078	0.10842
1.75	80.6666	0.510	0.03984	0.10641

The table presents the resultant torques, theoretical power, and power coefficient across a range of tip-speed ratios from 1 to 1.75. It's apparent that as the tip-speed ratio increases, the torque values decrease, reaching 0.510 × 10-3 N-m at a tip-speed ratio of 1.75, accompanied by an angular velocity of 80.6666 rad/s. However, despite the decrease in torque values, the power and power coefficient values exhibit some fluctuations. Notably, the power coefficient Cp, which is the focus, initially increases, then decreases at certain points. The maximum power coefficient Cp peaks at 0.108, occurring at a tip-speed ratio of 1.5. The corresponding graph depicting Cp against λ is provided below:

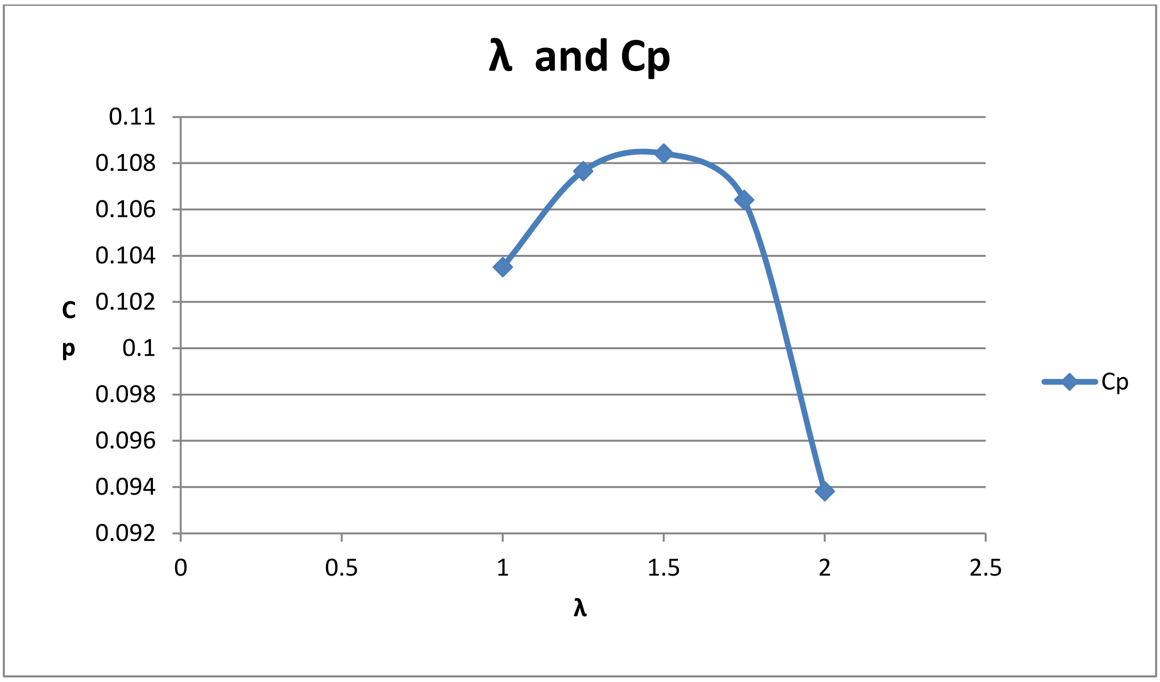

Figure III.11. Graph representing Cp Vs λ at pitch = 0.25R

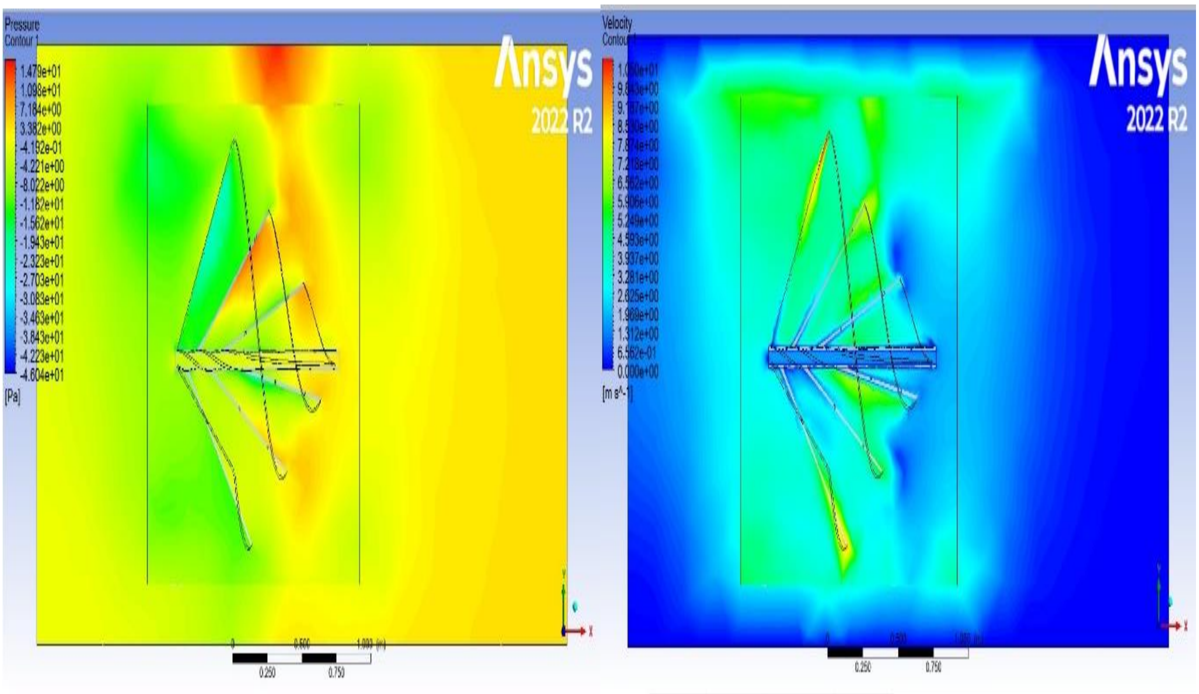

Figure III.12 Average velocity and Static pressure distribution field at pitch = 0.25R at central plane of turbine

Table III.4: Simulation data for different tip speed ratios at pitch =1.5R

λ	ω (rad/s)	T (× 10^{-3} N-m)	P (W)	C_p
1	45.6666	2.421	0.1089	0.2232
1.25	57.3333	2.134	0.1169	0.2405
1.5	70	1.865	0.1295	0.2461
1.75	80.6666	1.575	0.1141	0.2345

The table presents the resultant torques, theoretical power, and power coefficient across a range of tip-speed ratios from 1 to 1.75. It's apparent that as the tip-speed ratio increases, the torque values decrease, reaching 1.575 × 10-3 N-m at a tip-speed ratio of 1.75, accompanied by an angular velocity of 80.6666 rad/s. However, despite the decrease in torque values, the power and power coefficient values exhibit some fluctuations. Notably, the power coefficient Cp, which is the focus, initially increases, then decreases at certain points. The maximum power coefficient Cp peaks at 0.2461, occurring at a tip-speed ratio of 1.5. The corresponding graph depicting Cp against λ is provided below:

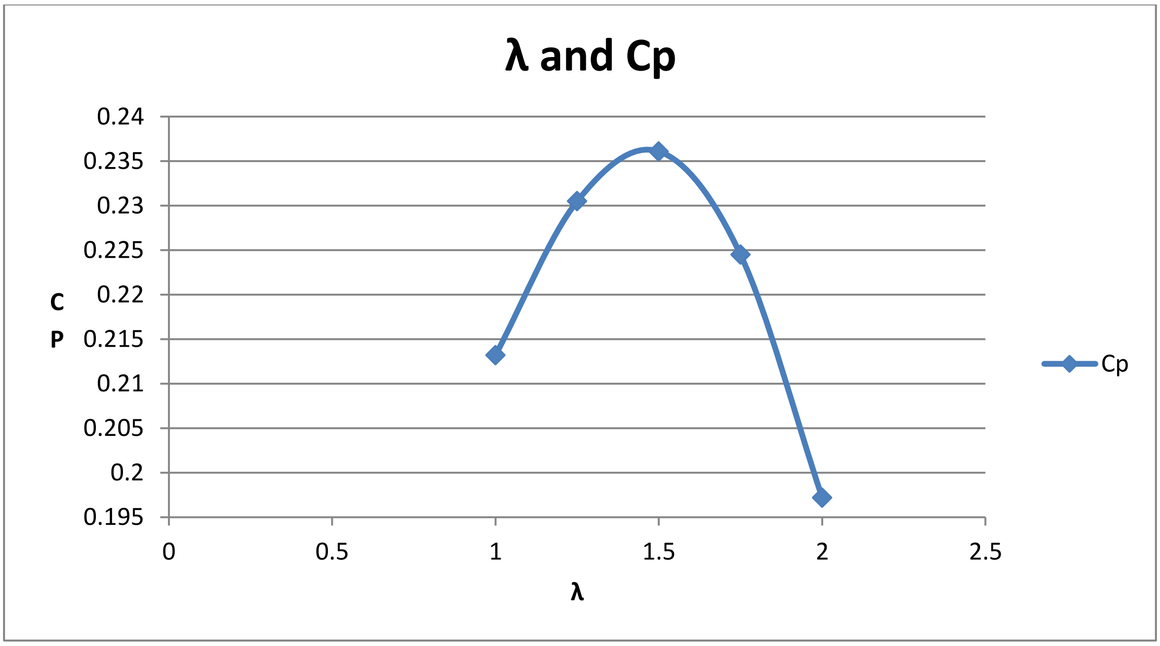

Figure III.13 Graph representing Cp Vs λ at pitch =1.5R

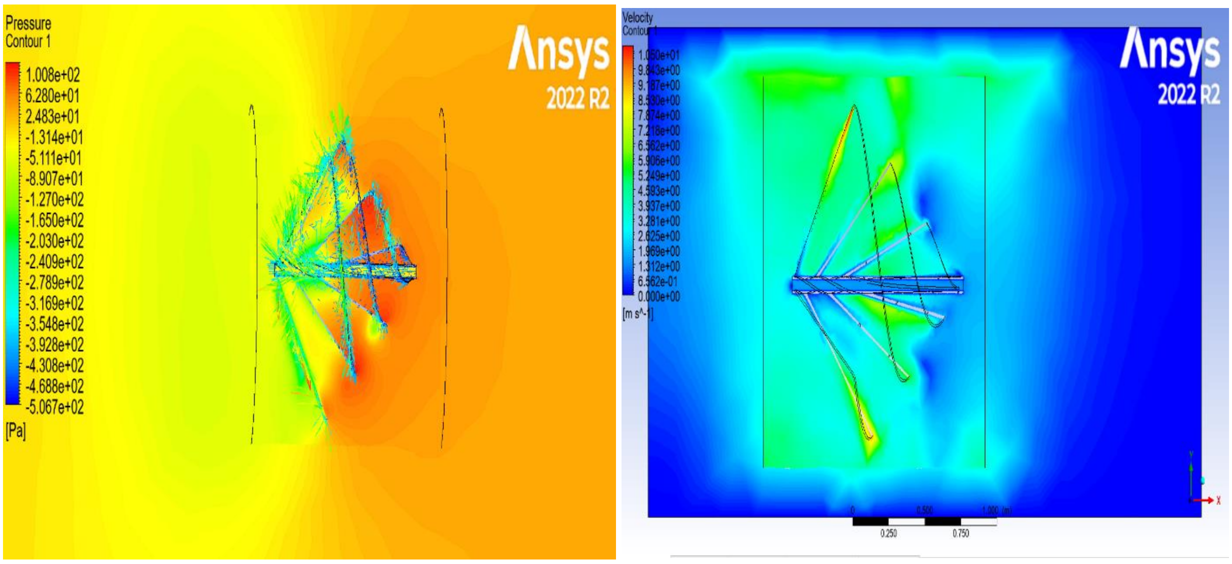

Figure III.14 Average velocity field and static pressure distribution at pitch = 1.5R at centralplane of turbine

Table **III**.5: Simulation data for different tip speed ratios at pitch = 2R

λ	**ω (rad/s)**	**T (× 10^{-3} N-m)**	**P (W)**	**C_p**
0.75	34	2.657	0.09072	0.2009
1	45.6666	2.208	0.10247	0.2151
1.25	57.3333	1.808	0.10584	0.2224
1.5	70	1.408	0.10011	0.2100

The table presents the resultant torques, theoretical power, and power coefficient for a range of tip-speed ratios from 0.75 to 1.5. As the tip-speed ratio increases, it's observable that the torque values decrease, reaching 1.408 × 10-3 N-m at a tip-speed ratio of 1.5, with a corresponding angular velocity of 70 rad/s. Despite the decrease in torque values, the power and power coefficient values exhibit some fluctuations. Initially, the power coefficient Cp increases, but at certain points, it starts to decrease. The maximum power coefficient Cp attains a value of 0.2224 at a tip-speed ratio of 1.25. The corresponding graph illustrating Cp against λ is provided below:

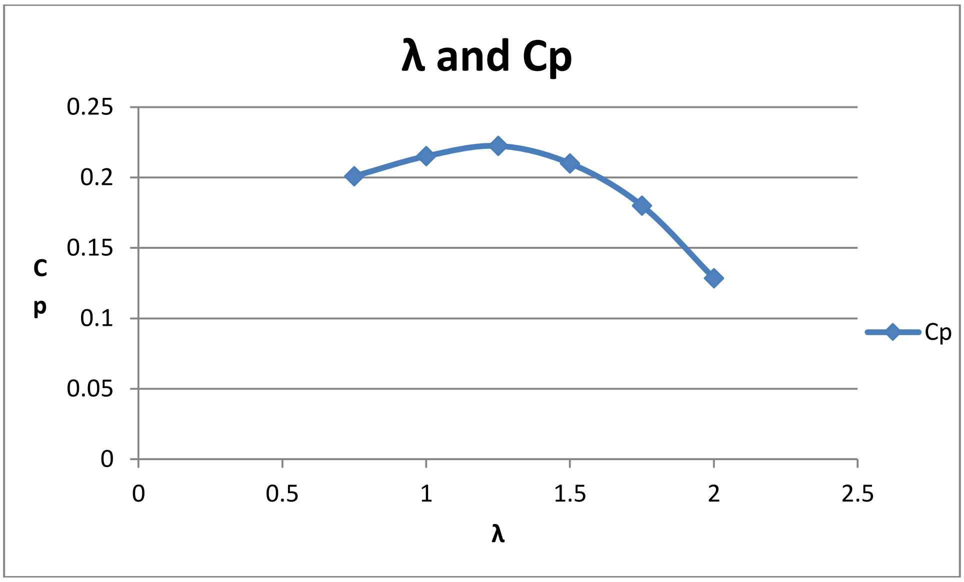

Figure III.15 Graph representing Cp Vs λ at pitch = 2R

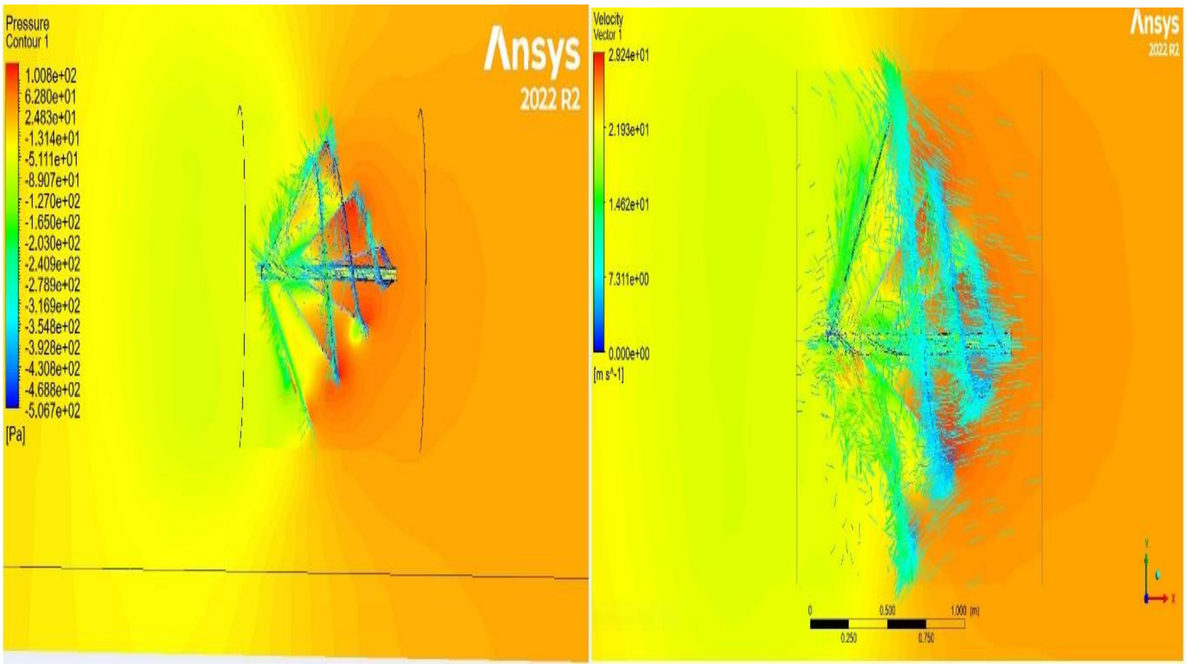

Figure III.16 Average velocity field and static pressure distribution at pitch = 2R at central Plane of turbine

After examining the data and graphs presented above, we determine the optimal pitch value where the maximum power coefficient is achieved, which is at a pitch of 1.5R at a tip speed ratio of 1.5.

Opening Angle

Now, the opening angles are varied from 30° and 60° to find out the optimum result.

Table **III**.6: Simulation data for different tip speed ratios at angle = 30°

λ	ω (rad/s)	T (× 10^{-3} N-m)	P (W)	C_p
0.75	34	2.270	0.08876	0.1797
1	45.6666	1.731	0.08942	0.1811
1.25	57.3333	1.183	0.07847	0.1575
1.5	70	0.672	0.05570	0.0984

The table presents the resulting torques, theoretical power, and power coefficients for tip-speed ratios ranging from 0.75 to 1.5. As the tip-speed ratio increases, torque values decrease, reaching 0.672 × 10-3 N-m at a tip-speed ratio of 1.5, with a corresponding angular velocity of 70 rad/s. Despite the decrease in torque values, power and power coefficient values exhibit some fluctuations. Initially, the power coefficient Cp increases, but then it starts to decrease at a certain point. The maximum power coefficient Cp is recorded at a value of 0.1811 for a tip-speed ratio of 1. The corresponding graph depicting Cp against λ is provided below:

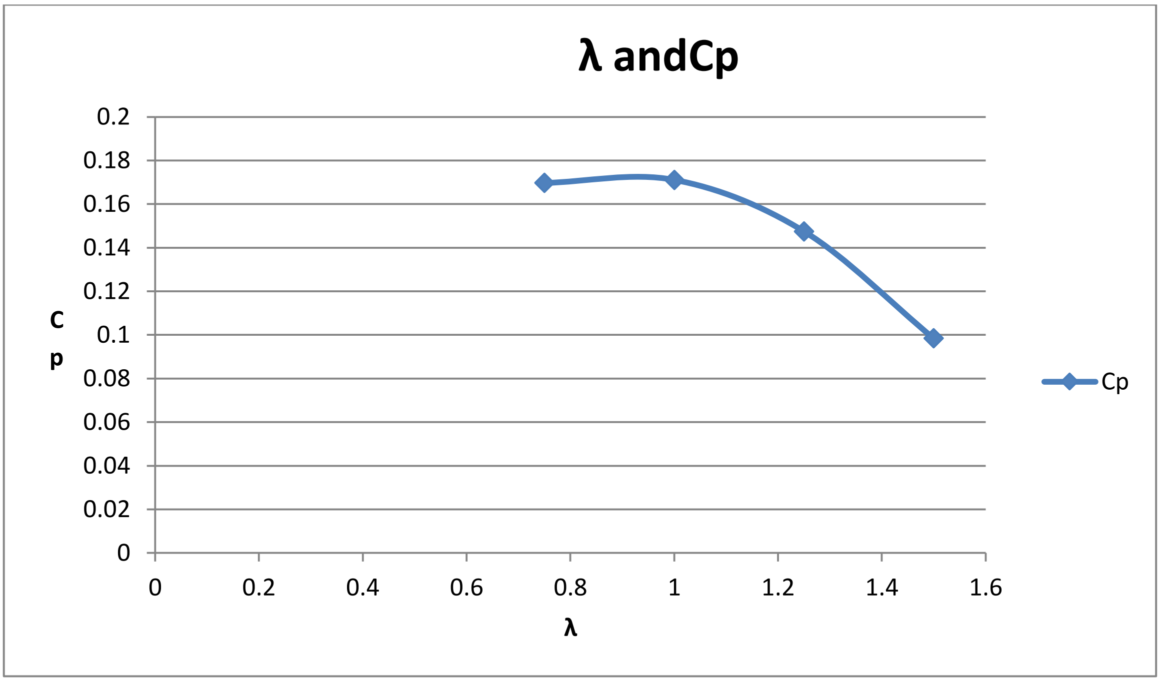

Figure III.17 Graph representing Cp Vs λ at opening angle at 30°

Table III.7: Simulation data for different tip speed ratios at angle = 60°

λ	**ω (rad/s)**	**T (× 10^{-3} N-m)**	**P (W)**	**C_p**
1	45.6666	2.121	0.0989	0.2432
1.25	57.3333	1.834	0.1069	0.2505
1.5	70	1.565	0.1095	0.2561
1.75	80.6666	1.275	0.1042	0.2445

The table displays the resulting torques, theoretical power, and power coefficients across a range of tip-speed ratios from 1 to 1.75. As the tip-speed ratio increases, the torque values decrease, reaching 1.275 × 10-3 N-m at a tip-speed ratio of 1.75, with a corresponding angular velocity of 80.6666 rad/s. However, despite the decrease in torque values, the power and power coefficient values exhibit some fluctuations. Initially, the power coefficient Cp increases, but then it starts to decrease at another point. The maximum power coefficient Cp is recorded at a value of 0.2561 for a tip-speed ratio of 1.5.

The corresponding graph between Cp and λ is given below:

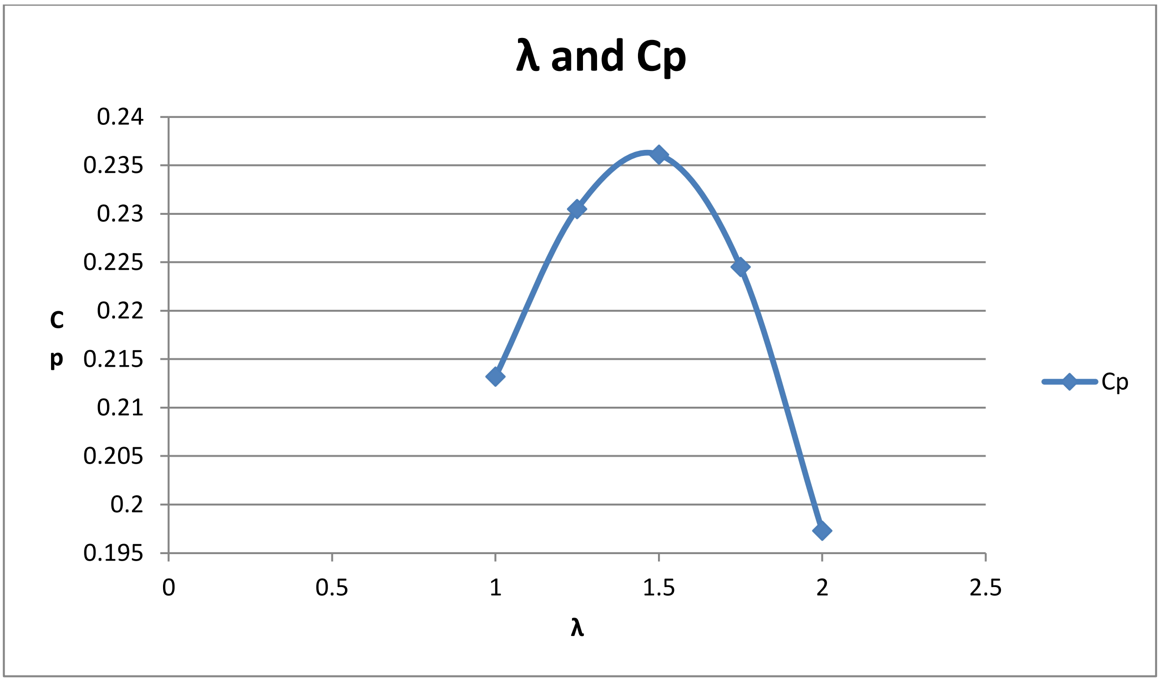

Figure III.18 Graph representing Cp Vs λ at opening angle at 60°

III.6.conclusion

In this chapter we used two simulation software which ANSNSY version 2022.R2 and solidworks version 2021. We designed a mini wind turbine and assumed our Study in a wind tunnel and we studied the behavior of the air around the blade in Different cases and we found that

Conclusion General

Conclusion générale

To analyse the torque characteristics of the Archimedes aerofoil wind turbine, Computational Fluid Dynamics (CFD) simulations were conducted under various wind and rotor speeds. The findings are summarized as follows:

Utilizing an aerofoil for the Archimedes wind turbine blade notably enhances torque at lower speeds, exhibiting an approximate 15% increase compared to the Archimedes Wind Turbine (AWT). This suggests its suitability for low and moderate wind speeds.

The study demonstrates that power output is intricately linked to both wind speed and the design parameters of the wind turbine blade.

The Archimedes aerofoil wind turbine proves capable of extracting more power than other wind turbines, particularly at lower and moderate speeds.

The use of both lift and drag forces obviates the need for electronic yawing equipment, thereby reducing costs associated with turbine operation.

CFD results indicate that the Archimedes aerofoil wind turbine shows promising potential for generating more power compared to other wind turbine designs, including the Archimedes spiral wind turbine.

Références

[1] F. Konig, Wind energy in parktischerNutzung, Munchen: UdoP friemer Verlag, 1978, p. 313-342.
[2] E. Fröde, Windmühlen, Köln: Du Mont Buchverlag, 1981.
[3] J. Notebaart, Windmühlen, Den Haag: Mouton-Verlag, 1972.
[4] “Wind-power-rennewalab-energy,” Oct 17, 2008. [Online]. Available: www.guardian.co.uk. [Accessed 03 28, 2017].
[5] Engineer's Technique D3960.
[6] E.Muldjadi, “Axial flux, modular, permanent-magnet generator with a toroidal winding for wind turbine applications,” at IEEE industry applications conference, 1998.
[7] [Online]. Available: http://tpe-si-2011.e-monsite.com/medias/images/eolhoriz3-2.jpg. [Accessed 03 28, 2017].
[8] JC.Sabonnadière, New energy technologies 1, Lavoisier, 2006.

[9] WWEA , [Online]. http://www.wwindea.org

10] O. GUERRI, “Wind Energy in Algeria,” Center for Development of Renewable Energies Ministry of Higher Education and Scientific Research

[12]A hands-on Introduction to Engineering Simulation. 1 June 2016 www.edx.org.
[13]Bakker, André. "Applied Computational Fluid Dynamics."
[14]Barrett, Sebastian Lachance and Edwin Corona. Fluent - Wind Turbine Blade. 10 June 2016 www.simcafe.org.
[15]Blazek, J. Computational Fluid Dynamics: Principles and Applications. Baden-Daettwil: ELSEVIER SCIENCE Ltd, 2001.
[16]Cao, Han. Aerodynamics Analysis of Small Horizontal Axis Wind Turbine Blades by Using 2D and 3D CFD Modelling. MSc Thesis. Preston, 2011.
[17]Chandrala, Mr. Monir, Abhishek Prof. Choubey and Bharat Prof. Gupta. Aerodynamic Analysis Of Horizontal Axis Wind Turbine Blade (2012).
[18]Eminoglu, Ulas and Saffet Ayasun. "Modeling and Design Optimization of Variable Speed Wind Turbine Systems." Energies (2014).

[19]M. Mieremet. "The aerodynamic method of the Archimedes Windturbine." Pusan National University, South Korea (2014).

[20]Namiranian, Abtin. 3D simulation of a 5MW wind turbine. Karlskrona, 2011.
[21**]**https://www.cadence.com/en_US/home/tools/system-analysis/computational-fluiddynamics/y-plus.html.